IMPROVING THE SOUND ABSORBING CAPACITY OF PORTLAND CEMENT CONCRETE PAVEMENTS USING RECYCLED MATERIALS

BY

JONATHAN GENE PITRE

Bachelor of Science, University of New Hampshire, 2000

THESIS

Submitted to the University of New Hampshire

in Partial Fulfillment of

the Requirements for the Degree of

Master of Science

in

Civil Engineering

May, 2007

This thesis has been examined and approved by.

_____

Thesis Director, Dr. David L. Gress, Professor of Civil Engineering

_____

Dr. Charles H. Goodspeed, Associate Professor of Civil Engineering

_____

Dr. Jo Sias Daniel, Assistant Professor of Civil Engineering

_____

Date

ACKNOWLEDGEMENTS

This project would not have been possible without the support of many people. I would like to thank the Recycled Materials Research Center and the Federal Highway Administration for the funding of the project. Many thanks to my adviser Dr. David Gress, along with my committee members Dr. Charles Goodspeed and Dr. Jo Daniel, who provided direction along the way. I also express my gratitude to Dr. Albert Frost who provided his assistance in constructing a laboratory manufactured impedance tube. Finally, thanks to my family, for their unwavering support throughout this process.

TABLE OF CONTENTS

LIST OF TABLES

LIST OF FIGURES

ABSTRACT

IMPROVING THE SOUND ABSORBING CAPACITY OF PORTLAND CEMENT CONCRETE PAVEMENTS USING RECYCLED MATERIALS

by

Jonathan Gene Pitre

University of New Hampshire, May, 2007

Over 50 percent of the United States population is exposed to traffic noise at a disturbance level of 70 decibel, while 15 percent are subjected to noise levels even higher and are considered an actual nuisance. Porous portland cement concrete pavements reduce noise at the source and have been very successful in Europe. A method was developed to predict the aggregate and concrete porosity and that was verified by image analysis. A laboratory manufactured impedance tube was developed to test the acoustical performance of the samples. Relationships were determined between the porosity, sample depth, aggregate type and acoustical performance. Detailed instructions were provided for a transportation agency to repeat the procedures described.

CHAPTER 1

INTRODUCTION

Noise issues become more of a problem as the population grows and communities are forced to move closer to highways. Approximately 50 percent of the United States population is exposed to noise levels beyond 70 decibel (the disturbance level), while 15 percent is subjected to noise levels of 85 decibel (the nuisance level).[1] Road traffic is the major source of noise as railroad and air traffic only account for one percent.[2]

It is becoming more common for highways to be designed with potential noise issues being taken into consideration. Many European countries have been designing roads with noise generation as a major design goal for many years. Now in the United States as populations grow, noise is rising to the top of highway specifications. Retrofitting existing highways for noise abatement is very costly. Noise barriers typically cost between $1 million and $1.5 million per mile.[3] This is why it is very important to prevent noise in the original design. A porous pavement reduces the amount of noise produced, so if there is less noise produced, that means less noise will travel to the surrounding communities.

Noise Generation on Portland Cement Concrete Pavements

Previous studies have determined there are two ways in which noise is generated on pavements, the engine/exhaust and tire-surface interface.[4,5] The engine and the exhaust generate the most obvious noise on pavements; however, noise is also generated on roads at the tire-surface interface. This is the primary focus of this research.

Engine-Exhaust

The type of exhaust system has a significant effect on the amount of noise produced depending on the vehicle type (truck, passenger car, etc.). Over the past 80 years there has been a 10 decibel decrease in noise generated from the power-train of automobiles due to better design, however there has been little or no reduction in noise generated by the tire-surface interface.[6] Tire-surface noise generated from increased traffic volume has drastically overwhelmed the minor 10 decibel decrease in noise generated from the power-train.

Tire-Surface Interface

Tire-surface noise is mainly a function of the characteristics of the tire (rubber, structure, treads and pattern), vehicle speed, and the pavement (surface roughness and porosity).[7]

The air movement in and out of the treads produces the noise from the tire-surface interface. Air enters the tread block and is forced out when the tire deforms upon contact with the pavement. This creates the process of air pumping. This phenomenon is mainly an air suction-and-expulsion that occurs in the hollows of the tire tread pattern and results in the tangential vibration of the tire tread blocks.[2] This action is responsible for frequencies greater than 1000 Hz. On a smooth surface, this action is increased because the air has no place to escape.

Tire deformation, as the pavement surface impacts the treads, causes vibration at the tire-surface interface at low frequencies below 1000 Hz.[2] Rough surfaces have a

major impact on noise production because the surface aggregate protrudes above the surface and causes more vibration to occur, as shown in Figure 1.

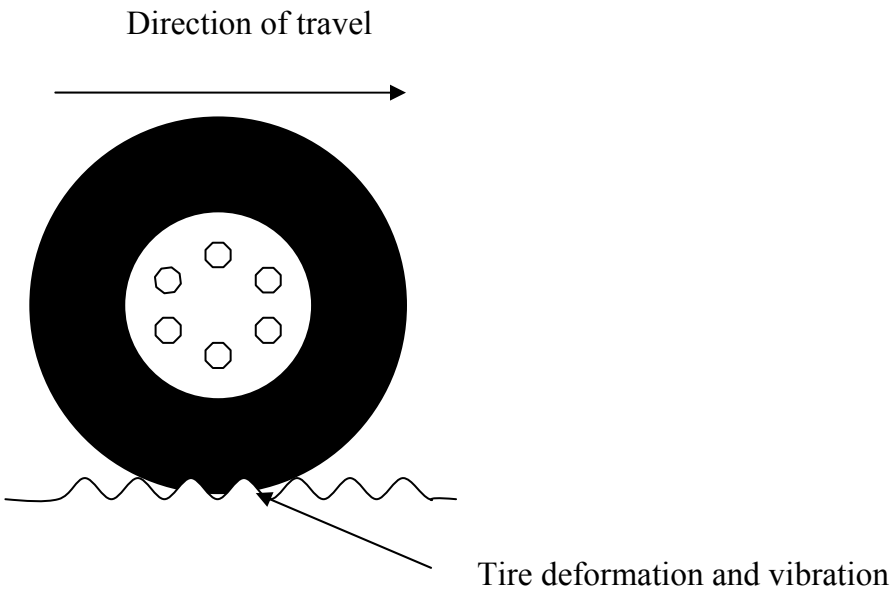

Figure 1 Tire vibration due to rough surface texture

The surface irregularities of PCC pavement can be categorized into four classes, microtexture, macrotexture, megatexture, and unevenness.[2] These are based on a range of characteristic dimensions along the surface that vary from a true planar surface. Microtexture, macrotexture, megataxture, and unevenness have the dimensions of less than 0.5 mm, 0.5 to 50 mm, 50 to 500 mm, and greater than 500 mm, respectively. Microtexture and unevenness have no direct affect on the amount of noise produced on a PCC pavement. Indirectly, unevenness can produce vibrations of the vehicles as well as of the ground. When vehicles vibrate the ground, they can vibrate nearby homes, which is a source of noise. Megatexture can be from the wear and tear of the PCC surface or

surface transverse wavelets. Macrotexture is a result of the aggregate projecting out of the PCC pavement surface or other surface treatments like grinding and grooving.[2] Another phenomena known as the "horn effect" actually amplifies noise at the tire-surface interface, which is illustrated in Figure 2.[2,7,8] A pocket shaped like a horn is created between the tire and pavement surface which influences wave-propagation resulting in a significant 10 – 20 decibel amplification.[8]

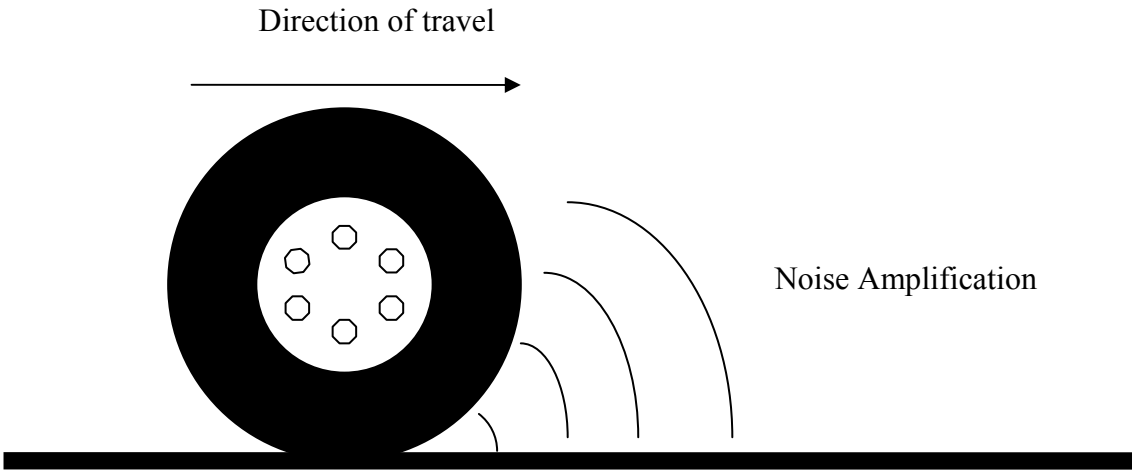

Figure 2 The horn effect

Noise Reduction on PCC Pavements

Three methods have been used to reduce noise on PCC pavements.[9] The first is to control the source of noise. This includes the automobile (engine and exhaust) and the tire and road interaction. Decreasing noise emitted from the source obviously reduces the overall noise on PCC pavements. Shielding the noise generated is the second way in

which noise can be reduced. The final method to reduce noise is to control noise propagation. Controlling the way the noise is transmitted can greatly decrease the amount of noise received.

Automobile

Legislation within the past ten years has greatly reduced the amount of noise that can be emitted from a vehicle's engine. Other laws also limit the amount of noise radiated from the exhaust system. One method that may be used to control the amount of noise from the source is to attach shields on the vehicle, reducing the amount of noise given off to the surrounding areas. This method is costly and with the quieter engines and exhausts of today, the focus has shifted to the two other ways of controlling noise.

Tire-Surface Interface

There have been proven methods of controlling the noise generated at the tire-surface interface. Many studies have investigated the application of different surface textures to the PCC pavement to both increase and reduce noise. Tining is a surface treatment that creates grooves in the pavement to allow surface water to drain off the pavement during rainy weather. Both uniform and random transverse tining provide higher noise levels than skewed longitudinal tining.[10] Uniform tining is used to make rumble strips along highways to intentionally create noise as a safety warning. The noise level increases with depth and width of the tining. It has been established that random spacing of grooves produces random frequencies, which prevents a singular frequency from spiking.[11,12,13] One of the limiting factors in tining is maintaining skid resistance. Transverse tining

allows water to escape in wet conditions preventing low speed vehicles from hydroplaning. Where very high speeds (130 km/h or greater) are expected, as in airports, longitudinal textures are used.[14]

Noise Interception

Noise barriers are used as common practice to change the way noise is received along the sides of PCC pavements. Noise barriers come in many sizes, shapes, and materials. A picture of a noise barrier is shown in Figure 3. Studies have shown when noise barriers are constructed on both sides of the road noise is effectively reduced.[15] This geometry allows multiple reflections of the noise which leads to dissipation through acoustic decay.

Another very effective proven methodology is to soundproof the surrounding buildings. This process was used in an air traffic area of Logan International Airport. Many of the surrounding homes installed extra insulation, improved the windows, and replaced doors with sound absorbing materials. Both of these methods work, however they are very costly to install and in the barrier case, it is not always aesthetically pleasing.

Figure 3 Noise barrier reducing noise entering residential community

Noise Propagation

Urethane, a 40 mm thick sound-absorbing material has been installed on the chassis of trucks near the sidewall of the tires. This method is only capable of reducing the noise slightly and other methods are probably more efficient.

An absorbent pavement in concept is capable of controlling the amount of noise propagated. The amplification produced by the horn effect is minimized and the air pumping effect is reduced because the air is evacuated inside the pores of the pavement structure.[7] A poro-elastic road surface was constructed with rubber as the main ingredient in a previous study, however wet friction, durability and adhesion affected its

functionality.[16,17] In partial-stone mixtures it has been shown that the macrotexture not flexibility reduces noise.[18]

Porous concrete layers have been evaluated as the top layer on PCC pavements.[19] This allowed the top surface to reduce the amount of noise propagated and generated. The bottom layer usually gives the overall strength of the system. This system can result in quiet and strong PCC pavements.

Porous PCC

The size, shape, and kind of aggregates used vary the amount of sound absorption.[20] Limestone compared to Basalt and Gritstone aggregates produces the highest maximum sound absorption peak due to high tortuosity and airflow resistivity values. The Woodside et al research suggests that smaller gaps between the aggregate produces higher airflow resistivity values, which in turn produces more sound absorbing mixtures.[20] The maximum size of the aggregate has a direct effect on porosity. Again, smaller aggregate sizes limit the gaps between the aggregate leading to improved sound absorption. To achieve the necessary strength requirements of the concrete mixture the size is usually limited to less than 9.5 mm. Aggregates with aspect ratios much larger than one, compared to cubic aggregate with aspect ratios of one, produce a higher maximum sound absorption.

A two-layer porous PCC can also be effective in reducing the amount of noise produced. The bottom layer of the system contains larger aggregate, typically 8-12 mm, while the top layer is composed of a smaller aggregate. This arrangement creates an

inkbottle effect, which allows sound waves to pass through the smaller pores in the top layer and bounces around in the larger pores of the bottom layer until the sound wave dissipates. A diagram of this system can be seen in Figure 4. The smaller pores in the top layer also prevent large debris from entering the pavement, minimizing clogging. Clogging reduces the sound absorbing capabilities of porous pavement.

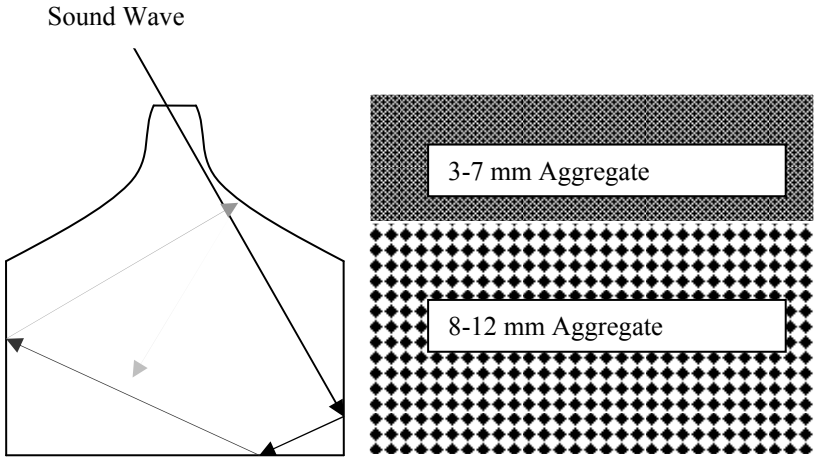

Figure 4 An inkbottle representing the sound dissipating effects of a two layer porous pavement

Desired Properties of Porous PCC Pavements

A small range of porosity in PCC pavements has been established from past work that is effective in reducing noise on pavements. In Japan, a porosity of 10.5 percent was used and a 6-8 decibel decrease was noticed.[2] In Germany, a porosity of 25 percent was used and a 4.3-7.0 decibel decrease was reported.[2]

Measuring porosity is an indirect way of relating pavement noise absorbing capabilities to mix proportions and is an ideal starting point in developing a viable sound absorbing concrete mixture. Ideally, sound absorption would be determined by laboratory testing using an impedance tube.

Since pavements fail in flexure, a modulus of rupture of 4.1-4.5 MPa is typically required at 28 days. To achieve this strength and to maintain the required porosity, additives such as silica fume and water reducers may be required. Durability of porous PCC pavements is a major issue. Some of the durability issues are plugging, resistance to freeze-thaw and deicing salts, and spalling.[2] Porous asphalt also has a similar problem of plugging. Plugging has little effect on the noise absorbing capacity, as was validated when the pores of a porous asphalt section were intentionally clogged and then cleaned and only a two decibel variation was noted.[21] The issue of water freezing inside the pores and then breaking apart the pavement is a concern, however with efficient drainage this problem can be overcome. It is very important that a sound absorbing pavement not be developed at the expense of sacrificing durability. To do so would be false economy as the overall costs of operation and maintenance would increase.

CHAPTER 2

MATERIALS AND METHODS

Significant properties of each material used in this research are provided and are examined for importance to the project. The methods used in examining the objectives of this study are discussed. Current testing procedures were used, however certain circumstances required the procedure to be modified or completely changed. A detailed description of the final procedure developed is presented for use by transportation agencies.

Materials

project was to incorporate recycled materials into the final mixture design. However, due to the limited amount of material obtained conventional aggregates were used to develop all procedures. To ensure both ends of the aggregate shape spectrum were covered, an angular and a rounded aggregate were evaluated. As previously stated, to meet the strength requirements for a porous pavement the aggregate size was limited to less than 9.5 mm. It was then decided the following sizes would be used to develop porous concrete pavements: 9.5 mm, 4.75 mm, and 2.36 mm.

To simplify the analysis most of the aggregate properties, such as number of fractured faces, surface area, modulus of elasticity, and porosity, were not determined. Each aggregate source was evaluated through the entire procedure developed. It was not practical to determine all aggregate properties, although some or all of those properties have the ability to influence the results obtained.

Cement

The cement used in this project was a basic Type I portland cement, which could be found at any building material supplier. The cement had the following chemical properties:

- C_3S – 55.0 percent
- C_3A – 10.0 percent
- MgO – 2.8 percent
- SO_3 – 2.9 percent
- Total Alkali – 1.0 percent
- Loss of Ignition – 1.0 percent

Conventional Aggregates

The two sources of conventional aggregates were used in this study because they were easily accessed and readily available. These aggregates are typically used in common construction practices in the area, such as asphalt paving and concrete.

Blue Rock

The angular material known as Blue Rock is quarried at Westbrook, Maine. The crushed stone gets its name from the blue-gray color. The 19.0 mm maximum size stone blend was sieved to gather the less than 9.5 mm aggregate size requirement to develop a porous pavement. All aggregate greater than 9.5 mm was then crushed and pulverized.

Figure 5 Blue Rock Aggregate

The blue rock has the following physical properties:

- Bulk Specific Gravity – 2.68
- Absorption – 1.0 percent

Newmarket

The rounded material known as Newmarket was excavated from open pits in Newmarket, New Hampshire. This material is obtained from a glacial deposit and therefore consists of rounded particles.

Figure 6 Newmarket Aggregate

The Newmarket aggregate had the following physical properties:

- Bulk Specific Gravity – 2.47
- Absorption – 0.8 percent

Recycled Aggregates

An effort was made to gather as many recycled aggregates as possible to incorporate as many different geographical regions. In some instances it may not be economical to use recycled aggregates if shipping is required, therefore examining multiple sources was considered a priority.

Blast Furnace Slag

Blast Furnace Slag, a recycled material, was obtained from Detroit, Michigan. A course aggregate, produced by crushing as waste product obtained by air cooling iron Blast Furnace Slag. It is a light brown to gray crystalline aggregate, formed simultaneously with the production of iron in a blast furnace. The particle sizes ranged from 25.0 mm to 4.75 mm. Once in the laboratory, the particles larger than 9.5 mm were then separated and crushed to produce the finer sizes.

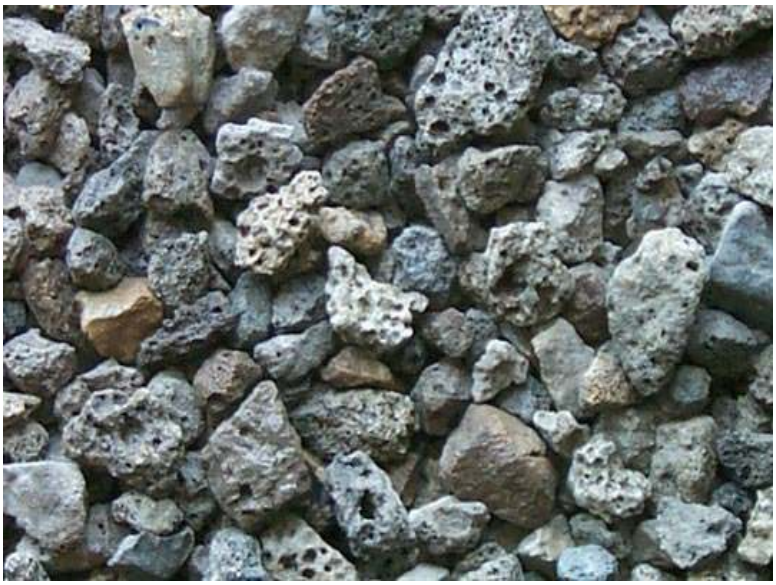

Figure 7 Blast Furnace Slag Aggregate

The blast furnace slag examined in this study had the following physical properties:

- Average Moisture – 2.3 percent
- Sum of Coke and Coal Particles – 0.1 percent (Specification 1.0 percent max)
- Freeze Thaw Dilation – 0.001 percent
- Loose Unit Weight – 1155.4 kg/m^3
- Rodded Unit Weight – 1328.3 kg/m^3
- Bulk Specific Gravity – 2.37
- Bulk Specific Gravity SSD – 2.46
- Absorption – 3.8 percent

Synthetic Lightweight Aggregate

Synthetic lightweight aggregate (SLA) is a blend of two products usually sent to disposal facilities, waste plastics and fly ash. The blend used for this project was 80/20 percent, fly ash and plastic, respectively.

The raw materials are blended and extruded into 50 mm by 9.5 mm thick strips. After the strips have cooled the material is granulated to form SLA, as shown in Figure 8. The grading for the SLA was 100 percent passing the 9.5 mm, 30 percent passing the 4.75 mm and zero percent passing the 2.36 mm.

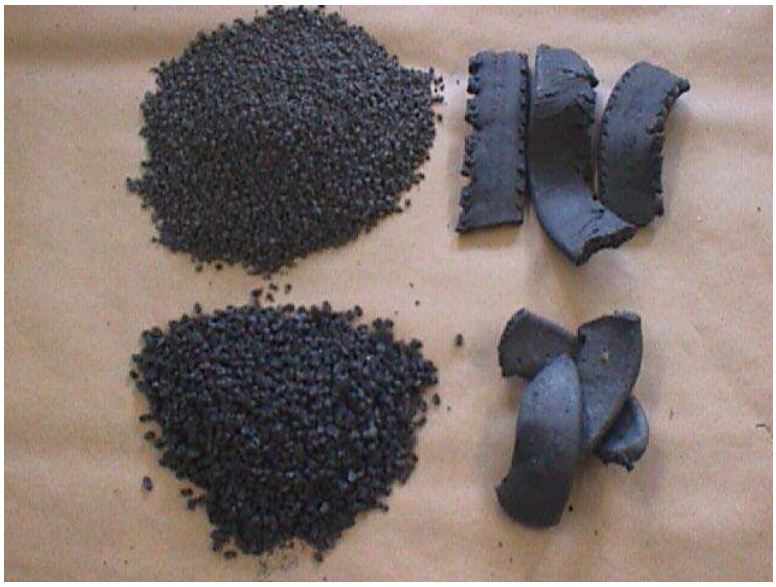

Figure 8 Synthetic Lightweight Aggregate strips and granulated

Recycled Concrete Aggregate

The recycled concrete aggregate (RCA) is composed of crushed 20 MPa concrete slabs. The concrete slabs had a water/cement ratio of 0.45.

Figure 9 Recycled Concrete Aggregate

Methods

The following section describes the methods used in determining the requirements set forth in this study.

Theoretical Aggregate Porosity

As stated previously porous concrete pavements develop there acoustic properties from the aggregate matrix. The logical place to start is to examine the porosity of a given volume of a vibrated grading of the aggregate being tested without portland cement paste. Once the aggregate porosity is determined a percentage of the voids can be filled with cement paste, thus giving a theoretical concrete porosity. An aggregate matrix is shown without and with the cement paste in Figure 10.

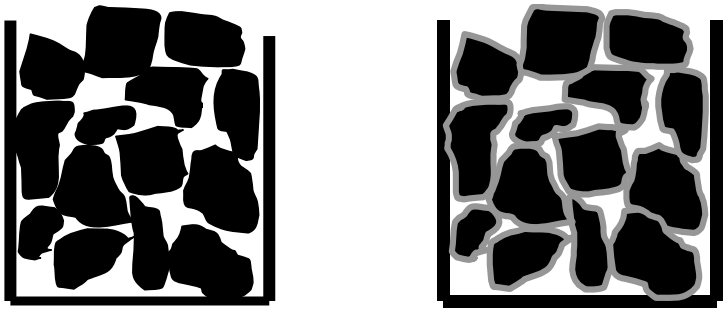

Figure 10 Aggregate matrix without and with cement paste

ASTM C29 Standard Test Method for Bulk Density and Voids in Aggregate was considered to determine the voids in the aggregate matrix, however some modifications were implemented to simplify the test.[22] The aggregate was blended in a 0.25 cubic meter portable concrete drum mixer. The blended aggregate was then placed in three equal lifts in a known volume steel bucket, which was calibrated according to ASTM C29. After each lift was placed the aggregate was compacted using a vibrating table, as shown in Figure 11. The amplitude and frequency of the vibrating table were adjusted to the point just below excessive excitation of the aggregate. Each lift was vibrated for 60 seconds. After the third lift was vibrated the bucket with aggregate was weighed, as shown in Figure 12.

Figure 11 Steel bucket placed on vibrating table

Figure 12 Steel bucket weighed

The bulk density was determined according to ASTM C29 and can be calculated as follows:

$$M = \frac{(G - T)}{V}$$

where:

M = bulk density of the aggregate, kg/m^3,

G = mass of the aggregate plus the measure, kg,

T = mass of the measure, kg,

V = volume of the measure, m^3.

The voids then can be calculated as follows:

$$\%\, Voids = 100\ \frac{[(S \times W) - M]}{(S \times W)}$$

where:

S = bulk specific gravity, ASTM C127 Standard Test Method for Specific Gravity and Absorption of Coarse Aggregate,[23] used to determine this,

W = density of water, 998 kg/m^3.

The porosity obtained by this method was verified independently by evaluating the voids inside the matrix. Red cement slurry was poured into the compacted aggregate in a 100 mm diameter and 200 mm tall cylinder. The cement slurry had a 0.6 water to cement ratio with super plasticizer to ensure it flowed into all pore space. Since ultimate strength was not a concern, the cylinder was placed in an oven at 60 degrees Celsius for 24 hours to achieve enough strength so the cylinder could be cut on a wet saw and polished on a polishing wheel using coarse to fine grit to achieve a smooth surface. A cut and polished section can be seen in Figure 13. The polished section was then placed directly on a flatbed scanner and captured into image analysis software. The image was then manipulated to convert the aggregate pieces into white pixels and the cement slurry into red pixels. An image of the converted image is presented in Figure 14. The percentage of red pixels was compared to the overall pixel count to determine the voids in

the aggregate matrix. This percentage was then compared back to the original voids percentage determined by the modified ASTM C29 procedure.

Figure 13 Cut and polished section of 4.75 mm Blue Rock Aggregate

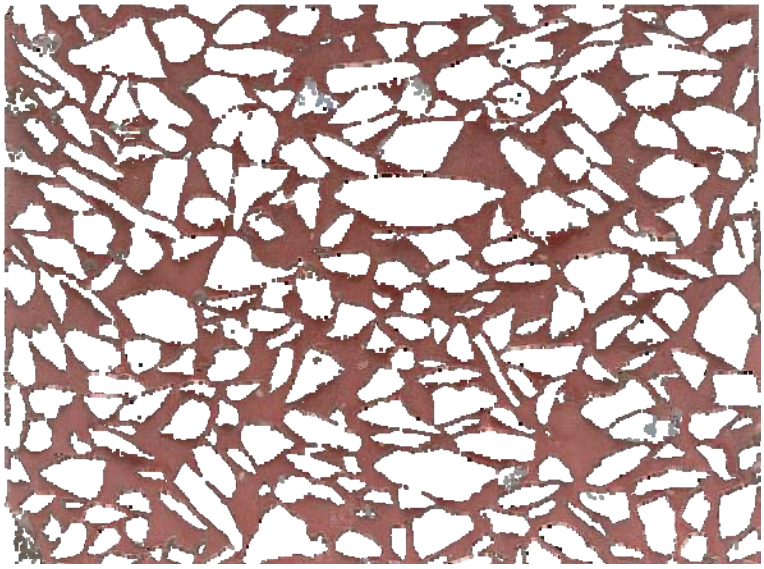

Figure 14 Pixelated image of 4.75 mm Blue Rock Aggregate

Mixture Proportioning

A plan to effectively evaluate the aggregate blends was needed to determine an optimum aggregate porosity. A simplex centroid statistical model was used to evaluate the porosity varying the aggregate blend composed of the previously determined aggregate sizes of 9.5 mm, 4.75 mm, and 2.36 mm. The simplex centroid is convenient since it only requires nine runs combinations to statistically represent the data, in which the center third point is repeated three times. The simplex centroid used in this part of the study is presented in Figure 15. Each aggregate source was individually evaluated as shown in Table 1 where the blend ID is listed for the Blue Rock and Newmarket aggregates. The ID represents a given aggregate source and the combination of aggregate sizes used in the individual trial. For example, BR-2.36/9.5 represents the Blue Rock aggregate source and is composed of a 50/50 percent by weight blend of 2.36 mm and 9.5 mm aggregate sizes.

Table 1 Aggregate blend ID's for optimum aggregate porosity

Aggregate Trial Percentage	**Blue Rock ID**	**Newmarket ID**
100% 2.36 mm	BR-2.36	NM-2.36
100% 4.75 mm	BR-4.75	NM-4.75
100% 9.5 mm	BR-9.5	NM-9.5
50% 2.36 mm - 50% 4.75 mm	BR-2.36/4.75	NM-2.36/4.75
50% 2.36 mm – 50% 9.5 mm	BR-2.36/9.5	NM-2.36/9.5
50% 4.75 mm – 50% 9.5 mm	BR-4.75/9.5	NM-4.75/9.5
33% 2.36 mm – 33% 4.75 mm – 33% 9.5 mm	BR-2.36/4.75/9.5	NM-2.36/4.75/9.5
33% 2.36 mm – 33% 4.75 mm – 33% 9.5 mm	BR-2.36/4.75/9.5	NM-2.36/4.75/9.5
33% 2.36 mm – 33% 4.75 mm – 33% 9.5 mm	BR-2.36/4.75/9.5	NM-2.36/4.75/9.5

Once the trials of the experiment were complete, an equation was developed for a particular aggregate. Proper proportioning the three aggregate sizes resulted in optimum aggregate matrix porosity. Now that an optimum aggregate porosity was determined cement paste could be added to the mixture to achieve a desired concrete porosity. The purpose of the cement paste was to evenly coat the aggregate with a thin layer to ensure the aggregate was bonded together. To achieve maximum porosity the fine aggregate was not utilized.

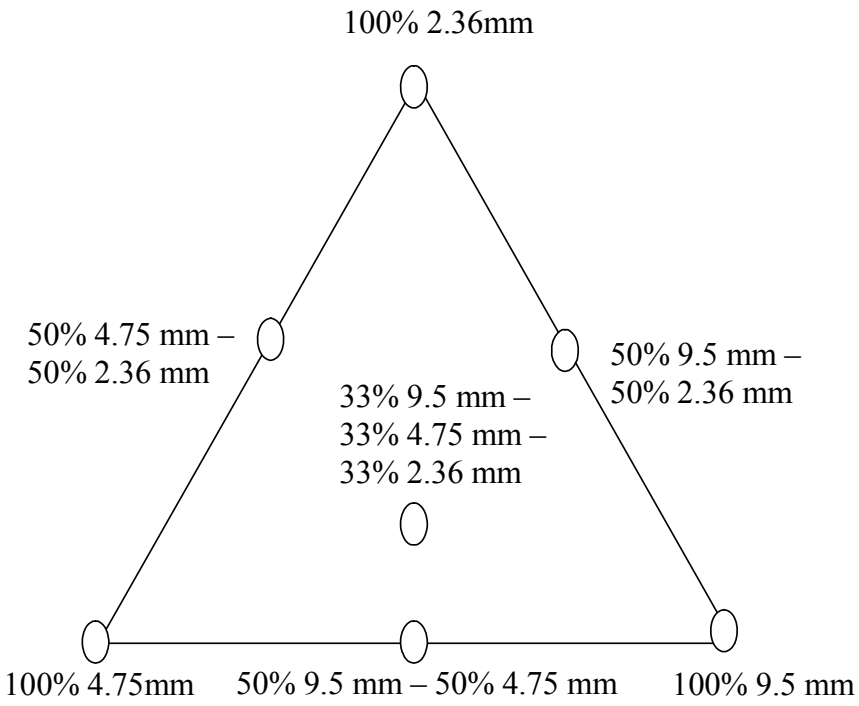

Figure 15 Simplex centroid used to determine optimum aggregate porosity

Batching

A five-gallon bucket mixer was used to batch the porous concrete components, as shown in Figure 16. The aggregate was placed in the bucket mixer first and blended for three minutes. After the aggregate was thoroughly blended portland cement was added and mixed for one minute. Water was then added slowly and mixed for five minutes. The plastic concrete was then distributed to beam or cylinder molds depending on what physical property was being considered. All molds were placed in two lifts and placed on the vibrating table to ensure maximum density was achieved. The molds were then struck off and covered with plastic and placed in a fog room at 22 degrees Celsius and 100 percent relative humidity for 24 hours. The molds were then stripped and the samples placed back in the fog room until tested.

Figure 16 Five-gallon bucket mixer

Testing

The section describes the tests used in determining the physical properties of porous PCC. In some instances, standard tests could be used to evaluate the physical properties, however other methods were adopted to effectively measure the desired properties.

Concrete Porosity Verification by Image Analysis

A method was developed to assure the desired porosity was achieved. At first glance, a volumetric measure method seemed to be the best way to do this, but after considering the concrete matrix may not have vital interconnected pores, this idea was abandoned. The image analysis method worked very well verifying the theoretical aggregate porosity so it was decided to adapt a similar process to determine the concrete porosity. After the concrete cylinder was cured it was cut and polished to examine the voids. The first thought was to dye the pores to differentiate between the aggregate and the pores, however a method to effectively accomplish this was not developed. A decision was made to fill the pores with a material that would infiltrate the pores, harden in a day or two, and have sufficient contrast to be optically distinguished.

Wood Putty® was found to be the best substance to meet the previously established requirements. A concrete sample filled with Wood Putty® in the pores is presented in Figure 17.

Figure 17 Concrete pores filled with Wood Putty®

The Wood Putty® was allowed about 1 hour to set. The concrete sample cut face was then washed to remove any excess Wood Putty® from the aggregate and allowed to harden 24 hours. The cut face was then placed on a polishing wheel to ensure the Wood Putty® was optically visible therefore identifying the pores. The polished face was then placed directly on a flatbed scanner and the procedure previously established was then followed. An enhanced image is shown in Figure 18.

Figure 18 Enhanced image

Acoustic Impedance Tube Properties

It is necessary to relate sound absorbing capabilities of the PCC pavement to concrete porosity and the aggregate being used. One way to measure the sound absorbing capabilities of the concrete is to use a sound impedance tube. Since this device was not available and the high cost to purchase a new one was not possible, alternative methods were considered. The advice of a well-respected Electrical Engineer, Professor Albert Frost, was used to manufacture a complicated but simple sound impedance tube.

Many factors can affect sound waves. The air temperature, relative humidity, and atmospheric pressure can change how fast the speed of sound travels. It should be understood that all data was collected under laboratory conditions.

Once the procedure was developed for constructing and using the UNH impedance tube a variety of samples were evaluated. It was only expected that the UNH impedance tube would have the ability to at least compare sample to sample, however select samples were chosen for calibration with a factory produced impedance tube located at Purdue University's Institute for Safe, Quiet, and Durable Highways.

The impedance tube was used to evaluate all variables, which could affect concretes ability to absorb sound. The following variables were evaluated,

- aggregate modulus of elasticity,
- sample depth,
- two-layer sample layer thickness (inkbottle),
- porosity,
- aggregate type (i.e. angular, rounded, etc).

One obvious physical aggregate characteristic examined was modulus of elasticity. To assure only the effect of Young's modulus was being evaluated the test aggregates had the same size, shape, and surface texture, while having a significant difference in modulus of elasticity. It was decided 12.5 mm glass, plastic, and steel balls would be used to analyze the effect of modulus of elasticity. The glass, plastic, and steel balls had a module of 72, 2, and 200 GPa, respectively.

Theory

An impedance tube is composed of a speaker, tube, microphone and a sample holder. A sound wave is generated from the speaker and then travels down the tube to the sample. The sound is either absorbed by the sample or reflected back down the tube. The microphone collects the two waves in the sound impedance tube, the one generated by the speaker and the one reflected by the sample. The analysis of the acoustics inside the tube can be mathematically simplified. The general equation for a sound wave, p, is:

$$p = A \sin 2\pi \left(\frac{t}{T} - \frac{x}{\lambda}\right)$$

where:

A = pressure amplitude

t = time

T = period

x = distance

λ = wavelength

The two waves in the tube can be written in the following way:

$$p_{generated} = A_{+} \sin 2\pi \left(\frac{t}{T} - \frac{x}{\lambda}\right)$$

$$p_{reflected} = A_{-} \sin 2\pi \left(\frac{t}{T} + \frac{x}{\lambda}\right)$$

A profile of the two waves is shown in Figure 19. When the two waves produce a maximum the equation can be written as:

$$A_{\max} = A_{+} + A_{-}$$

When the two waves produce a minimum the equation can be written as:

$$A_{\min} = A_{+} - A_{-}$$

A maximum and minimum can also be written as:

$$A_{\max} = A_{+} + nA_{+}$$

$$A_{\min} = A_{+} - nA_{+}$$

where:

n = reflection coefficient

When A_{max} is divided by $A_{min,}$ the result is as follows:

$$\frac{A_{\max}}{A_{\min}} = \frac{A_{+} + nA_{+}}{A_{+} - nA_{+}} = \frac{1+n}{1-n}$$

Solving for n:

$$n = \frac{A_{\max} - A_{\min}}{A_{\max} + A_{\min}}$$

The sound absorption coefficient, α, is defined as:

$$\alpha = 1 - |n|^2$$

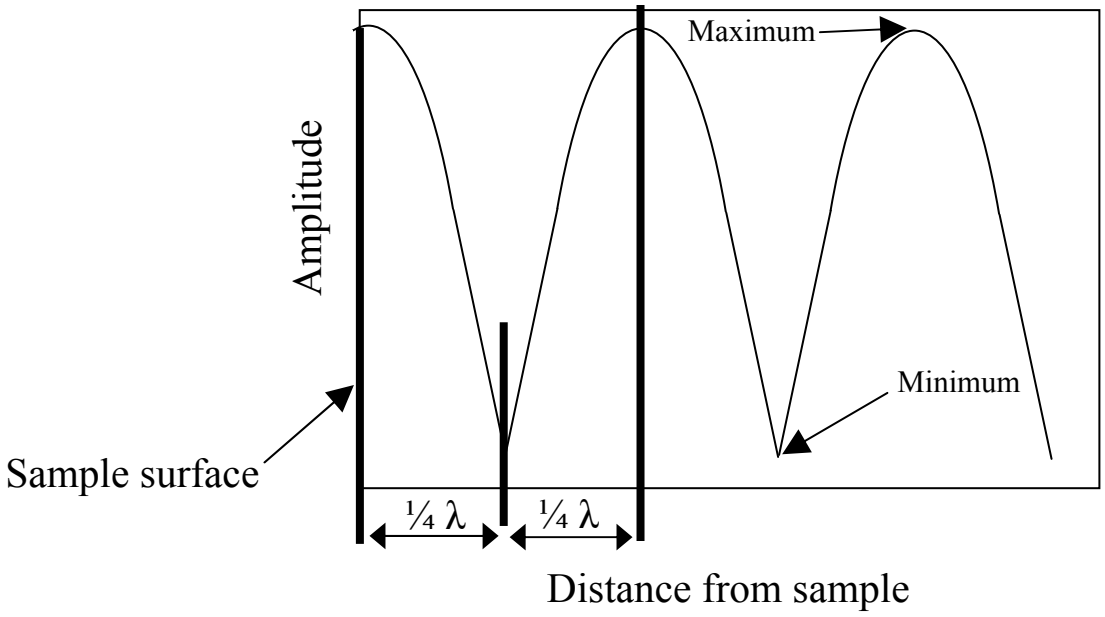

Figure 19 Theoretical profile of the generated and reflected wave

Development

The sound impedance tube was made using a 101 mm diameter by 2.45 m long PVC pipe. A digital frequency generator was used to produce a sinusoidal sound wave, which was amplified to a measurable level. The sound wave was generated through an 89 mm diameter speaker. Sound waves travel from the speaker through the pipe to the sample, where some are absorbed and some are reflected back. A microphone captures the reflected and original sound waves. A frequency filter maximizes the two waves before being measured on an oscilloscope. Fiberglass insulation is located immediately after the speaker to prevent the reflected sound from reflecting off the speaker and back to the sample. A reference material, which in theory reflects 100 percent of the sound wave, was used behind the sample to ensure the system was closed. The electronic equipment is presented in Figure 21.

According to ASTM C 384 Standard Test Method for Impedance and Absorption of Acoustical Materials by Impedance Tube Method, there are restrictions on the length and diameter of the impedance tube.[24] The range of frequencies used were 300 to 1500 Hz. The following restrictions comply with the ASTM C384 standard. The first restriction applies to the diameter of the tube.

$$d < 0.586\frac{f}{c}$$

where:

d = diameter of tube (m)

f = frequency (Hz)

c ≈ speed of sound in air, 343 m/s (19° Celsius, 101 kPa pressure, and 50 percent relative humidity)

As stated above the lowest frequency that will be used is 300 Hz.

$$d < 0.586\frac{300Hz}{343m/s} = 0.513m$$

The diameter of the tube was within the restriction, 0.101 m < 0.513 m.

The second restriction applied to the length of the tube was:

$$3\frac{\lambda}{4} < l - d$$

where:

λ = wavelength (m)

l = length of tube (m)

d = diameter of tube (m)

Solving for l and substituting for wavelength of 300 Hz.

$$l > 3\frac{1.13m}{4} + 0.101m = 0.951m$$

The length of the tube was within the restriction, 2.45 m > 0.95 m.

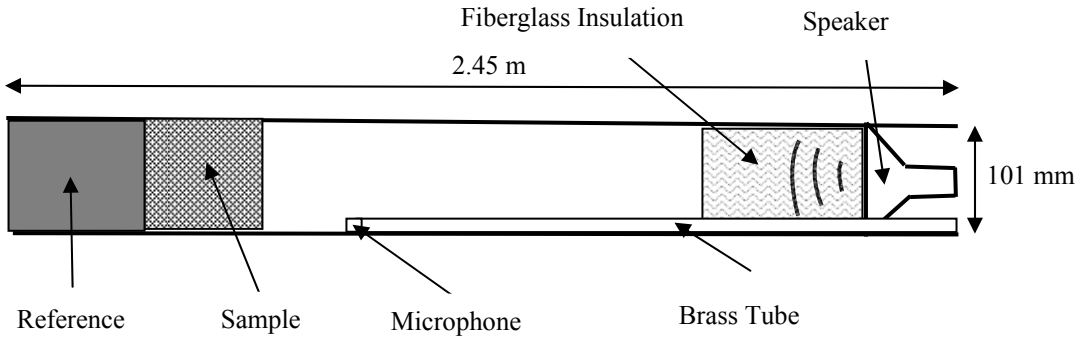

Figure 20 Sound impedance tube

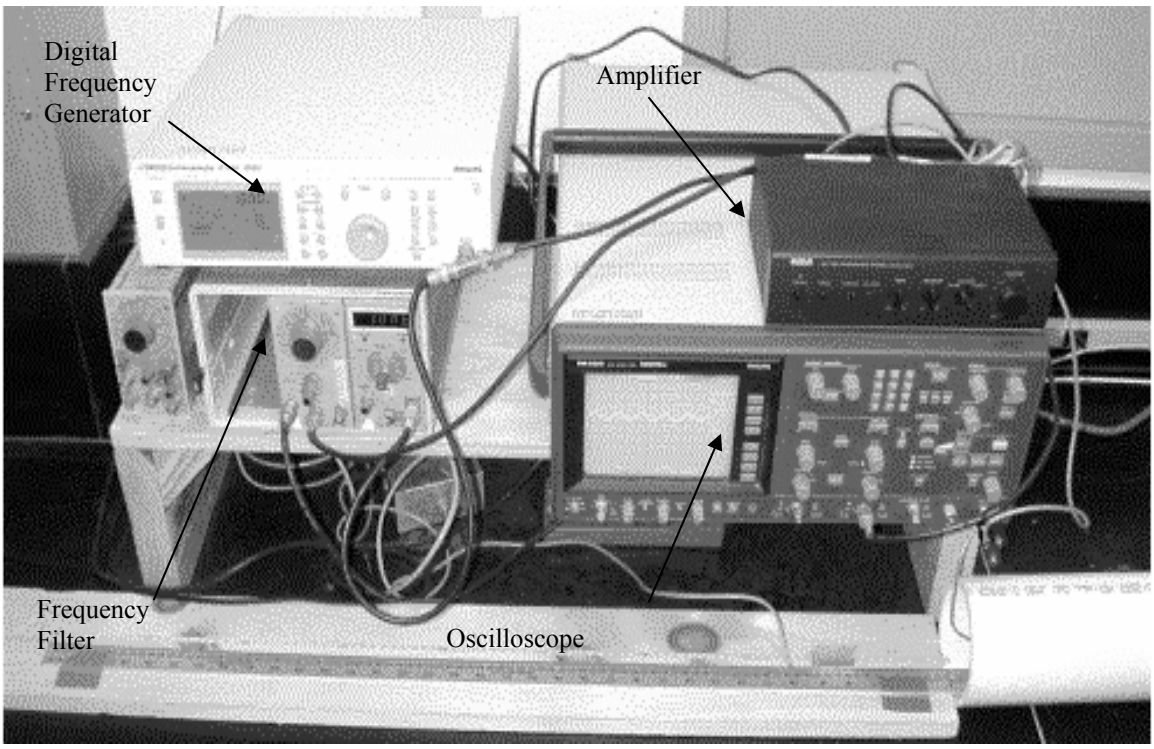

Figure 21 UNH impedance tube electronic equipment

A procedure was developed to ensure consistent data could be obtained with the UNH sound impedance tube. The important issues considered in developing a procedure were:

- the type of material behind the sample,
- sensitivity to sample placement,
- the number of replications.

Three different setups were evaluated to simulate field conditions. The first, shown in Figure 22, is the UNH impedance tube with no material behind the sample. This configuration does not mimic field conditions because in reality the concrete would have a base material, which would be expected to absorb and reflect some of the sound back through the sample.

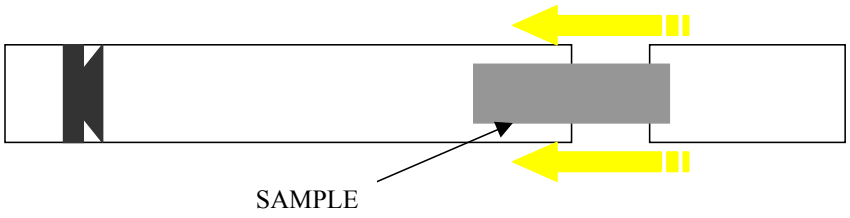

Not to scale

Figure 22 UNH impedance tube with no backing material

The second setup evaluated crushed gravel placed behind the sample, as shown in Figure 23. The crushed gravel was 19 mm Blue Rock, a typical pavement base material.

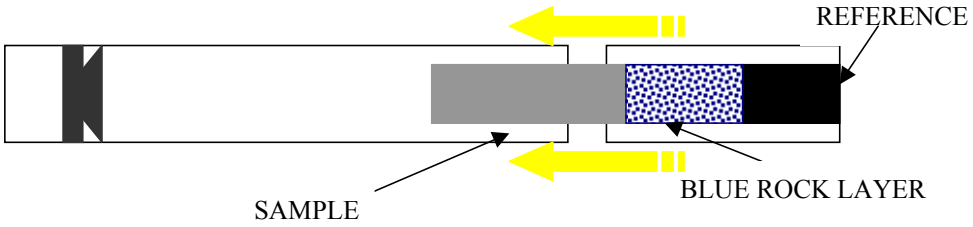

Not to scale

Figure 23 UNH impedance tube with crushed gravel backing material

The third setup, shown in Figure 24, has a reference material placed behind the sample. Perfect reference material should reflect nearly 100 percent of the generated signal. Theoretically, the impedance tube is a closed system, therefore it does not take into account any losses from the reference material

absorbing the generated signal or the generated signal escaping the tube. Three reference materials were selected to examine the reflective properties:

- "Paste": portland cement paste, with a water/cement ratio of 0.3, and a superplasticizer, 100 mm diameter x 200 mm long
- "Paste + Glass": Made with the above paste and crushed glass (50 percent cement / 50 percent glass), 100 mm diameter x 200 mm long
- "Ultra-high density Polyethylene": Polyethylene very high density cylinder, 100 mm diameter, 250 mm long

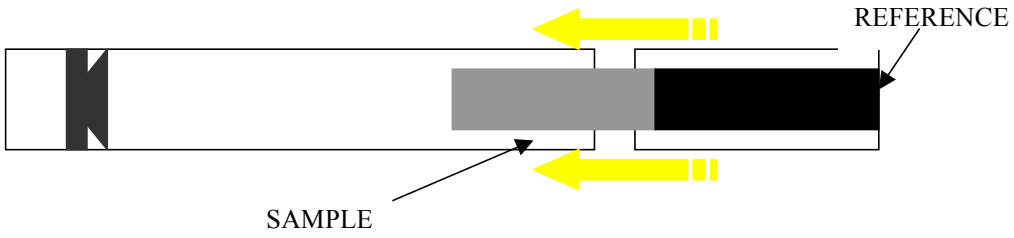

Not to scale

Figure 24 UNH impedance tube with reference backing material

The effect of position and angle of the surface of the sample was evaluated to see their influence on test results. The samples were placed in the UNH impedance tube and rotated a quarter turn to quantify the significance of changing the orientation of the sample.

The precision obtained measuring the amplitude of the signal with the oscilloscope was 10 mV. The signal was 5 mV wide producing an error in measuring the absorption coefficient defined as:

$$\frac{\partial \alpha}{\alpha} = \frac{40 \times A_{\min}}{(A_{\max} + A_{\min})(A_{\max} + A_{\min})}$$

To quantify the error in measuring the amplitude of the signal two different speakers were examined. Both a 15 and 25-watt speaker were used to compare the error in measuring the amplitude of the signal. A higher-powered speaker produces larger amplitudes, thus reducing the error in measuring the absorption coefficient. For statistical purposes, three sets of measurements were taken to obtain an average error.

Pulse Velocity

The principle of the device used to measure pulse velocity is simple: a transmitter generating a pulse is placed at one end of the sample, while a receiver collects the signal at the other end. The speed of the pulse inside the sample is then given by the time the signal takes to go from the transmitter to the receiver through the length of the sample. An illustration of the setup is presented in Figure 25. Pulse velocity has been measured in accordance to ASTM C597 Standard Test Method for Pulse Velocity Through Concrete.[25]

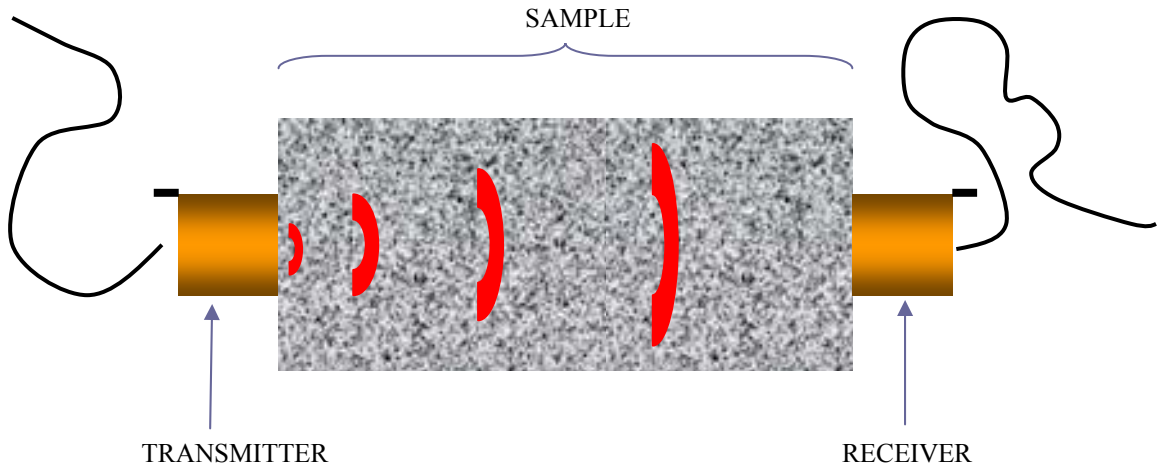

The significance of the pulse velocity was to determine if testing results were skewed due to varying sample matrix. Figure 26 pictorially shows a sample with good and poor contact. Pulse velocity relies on surface contact to produce quality results, and if the transducers do not have proper surface contact, the results are expected to be variable and inaccurate.

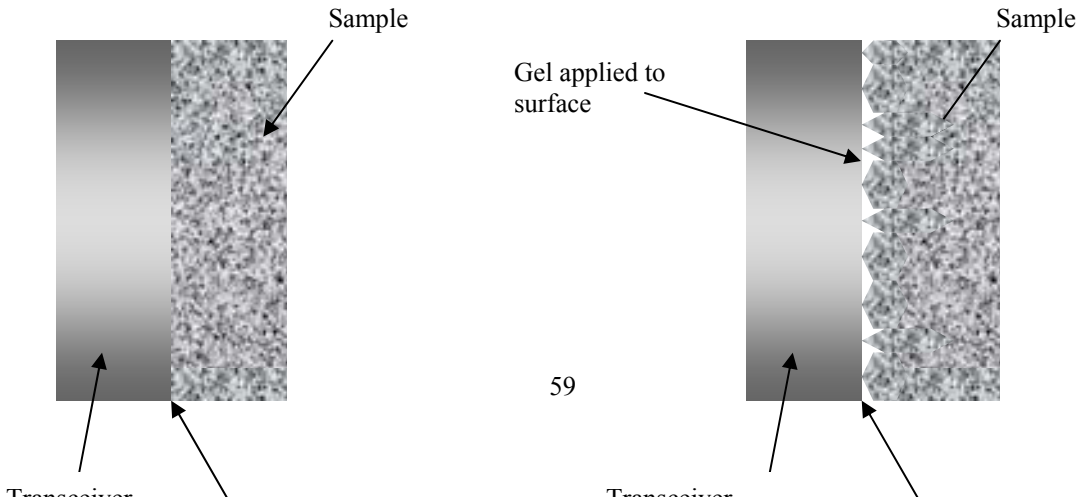

Figure 26 Pulse velocity contact surface

Flexural Strength

Rigid pavements are designed by specifying a given concrete's flexural strength. Obtaining a adequate flexural strength of a porous PCC was predicted to be problematic. Minimum flexural strengths vary for rigid pavements between 3.8 and 4.5 MPa. ASTM C78, Standard Test Method for Flexural Strength of Concrete (Using Simple Beam with Third-Point Loading) was used to determine the flexural strength of the samples.[26] The molds used in this test were 101 by 280 mm.

Compressive Strength

The compressive strength of the samples was examined for informational purposes. The flexural strength is the controlling property of pavement design, therefore the compressive strength was only tested on a few samples. The compressive strength was examined in accordance to ASTM C39 Standard Test Method for Compressive Strength of Cylindrical Concrete Specimens.[27]

CHAPTER 3

RESULTS AND DISCUSSION

Theoretical Aggregate Porosity

The theoretical aggregate porosity of Blue Rock Aggregate compacted as per the specification of modified ASTM C29 is presented in Table 2.

Table 2 Blue Rock Aggregate theoretical porosity

Blend ID	Theoretical Aggregate Porosity
BR-2.36	41.5%
BR-4.75	42.3%
BR-9.5	43.7%
BR-2.36/4.75	36.5%
BR-2.36/9.5	40.6%
BR-4.75/9.5	39.9%
BR-2.36/4.75/9.5	39.1%
BR-2.36/4.75/9.5	37.7%
BR-2.36/4.75/9.5	41.5%

The statistical equation for the theoretical porosity is:

$$porosity = 41.5\alpha + 42.3\beta + 43.7\chi - 21.6\alpha\beta - 8\alpha\chi - 12.4\beta\chi + 43.2\alpha\beta\chi$$

$R^2 = 0.82$

where:

α = the proportion of 2.36 mm aggregate

β = the proportion of 4.75 mm aggregate

χ = the proportion of 9.5 mm aggregate

$\alpha + \beta + \chi = 1$

The equation can be used to predict the porosity of Blue Rock Aggregate only, for example for a blend of proportions 0.40 of 2.36 mm, 0.25 of 4.75 mm, and 0.35 of 9.5 mm the theoretical aggregate porosity of Blue Rock Aggregate would be 39.6 percent.

In Table 3, the theoretical aggregate porosity for Newmarket Aggregate is presented from the modified ASTM C29.

Table 3 Newmarket Aggregate theoretical porosity

Blend ID	**Theoretical Aggregate Porosity**
NM-2.36	30.6%
NM-4.75	34.5%
NM-9.5	36.3%
NM-2.36/4.75	32.9%
NM-2.36/9.5	34.0%
NM-4.75/9.5	34.0%
NM-2.36/4.75/9.5	32.9%
NM-2.36/4.75/9.5	32.4%
NM-2.36/4.75/9.5	32.2%

Similarly, to the Blue Rock Aggregate an equation was developed to calculate the theoretical aggregate porosity by blending the selected aggregate sizes. The porosity can be predicted by the following equation:

$$porosity = 30.6\alpha + 34.5\beta + 36.3\chi + 1.4\alpha\beta + 2.2\alpha\chi - 5.6\beta\chi - 29.1\alpha\beta\chi$$

$R^2 = 0.99$

where:

α = the proportion of 2.36 mm aggregate

β = the proportion of 4.75 mm aggregate

χ = the proportion of 9.5 mm aggregate

$\alpha + \beta + \chi = 1$

The theoretical aggregate porosity can be predicted for any aggregate using the above procedure. Determining the aggregate porosity without a cement matrix is the starting point when designing a given desired concrete porosity. Once the aggregate porosity is determined the cement paste content can be adjusted for aggregate availability and strength requirements. For instance, if an aggregate supplier only has 9.5 mm and 4.75 mm aggregate sizes available this would limit the possible combinations that could be used in the mixture design. The mixture designer would assign the proportion of 2.36 mm, α, zero, which then would allow the designer to only use 9.5 mm and 4.75 mm.

In Table 4, the theoretical aggregate porosity is compared to the image analysis results for Blue Rock Aggregate.

Table 4 Blue Rock Aggregate theoretical and image analysis porosity

Blend ID	**Theoretical Aggregate Porosity**	**Image Analysis Porosity**
BR-2.36	41.5%	47.2%
BR-4.75	42.3%	41.7%
BR-9.5	43.7%	39.4%
BR-2.36/4.75	36.5%	41.3%
BR-2.36/9.5	40.6%	41.5%
BR-4.75/9.5	39.9%	44.0%
BR-2.36/4.75/9.5	39.1%	37.2%
BR-2.36/4.75/9.5	37.7%	37.2%

BR-2.36/4.75/9.5	41.5%	37.2%

Matched pair analysis was used to determine the difference between the aggregate theoretical porosity and image analysis porosity. Sample paired observations are randomly selected from the target population of paired observations. The assumption that the population of paired differences is normally distributed for this analysis is reasonable. A confidence interval was calculated to determine if zero falls within that interval. If zero falls within that interval there is insufficient evidence to conclude there is a difference between the two means. The confidence interval of a paired observation analysis is defined as:

$$\bar{d} \pm t_{\frac{\alpha}{2}} \left(\frac{s_d}{\sqrt{n}} \right)$$

where:

$\bar{d}$ = the mean of the matched pair differences

n = the number matched pair differences

s_d = the standard deviation of the matched pair differences

$t_{\frac{\alpha}{2}}$ = a value from the Student's t distribution based on (n-1) degrees of freedom

α = the values outside the specified interval of the Student's t distribution

Table 5 Blue Rock Aggregate difference between the theoretical porosity and image analysis porosity values

Blend ID	Theoretical Aggregate Porosity	Image Analysis Porosity	Difference Between Values

BR-2.36	41.5%	47.2%	-5.7%
BR-4.75	42.3%	41.7%	0.6%
BR-9.5	43.7%	39.4%	4.3%
BR-2.36/4.75	36.5%	41.3%	-4.8%
BR-2.36/9.5	40.6%	41.5%	-0.9%
BR-4.75/9.5	39.9%	44.0%	-4.1%
BR-2.36/4.75/9.5	39.1%	37.2%	1.9%
BR-2.36/4.75/9.5	37.7%	37.2%	0.5%
BR-2.36/4.75/9.5	41.5%	37.2%	1.5%

A 95 percent confidence interval was used to determine if there was insufficient evidence to conclude there was a difference between the two means.

$\bar{d}$ = -0.74

n = 9

s_d = 3.41

α = 0.05

$t_{\frac{\alpha}{2}}$ = 2.306

The 95 percent confidence interval is:

-0.74 ± 2.62

It is estimated with 95 percent confidence that the difference between the Blue Rock theoretical aggregate porosity and the image analysis porosity falls within the interval from -3.36 to 1.87. Since zero is within the interval, there is insufficient evidence to conclude there is a difference between the means suggesting there is no difference between the two methods of determining porosity.

Similarly, the Newmarket aggregate results were evaluated to determine if the theoretical aggregate porosity was equivalent to the image analysis porosity.

Table 6 Newmarket Aggregate difference between the theoretical porosity and image analysis porosity values

Blend ID	Theoretical Aggregate Porosity	Image Analysis Porosity	Difference Between Values
NM-2.36	30.6%	32.1%	-1.5%
NM-4.75	34.5%	37.5%	-3.0%
NM-9.5	36.3%	31.0%	5.3%
NM-2.36/4.75	32.9%	29.2%	3.7%
NM-2.36/9.5	34.0%	34.5%	-0.5%
NM-4.75/9.5	34.0%	33.7%	0.3%
NM-2.36/4.75/9.5	32.9%	31.0%	1.9%
NM-2.36/4.75/9.5	32.4%	28.1%	4.3%
NM-2.36/4.75/9.5	32.2%	31.9%	0.3%

The 95 percent confidence interval is:

1.2 ± 2.04

It was estimated with 95 percent confidence that the difference between the Newmarket theoretical aggregate porosity and the image analysis porosity falls within the interval of -0.84 to 3.24. Since zero is within the interval, there is insufficient evidence to conclude there is a difference between the means.

The statistical analysis on the control aggregates showed that the theoretical aggregate porosity was acceptable for estimating the aggregate porosity. In Table 7 through Table 9, the theoretical aggregate porosity is shown for the recycled aggregates discussed in previous sections. In addition, following the tables are the equations that can predict the porosity for any given combination.

Table 7 Blast Furnace Slag Aggregate theoretical porosity

Blend ID	**Theoretical Aggregate Porosity**
BFS-2.36	36.5%
BFS-4.75	39.6%
BFS-9.5	43.1%
BFS-2.36/4.75	35.8%
BFS-2.36/9.5	41.2%
BFS-4.75/9.5	33.4%
BFS-2.36/4.75/9.5	36.3%
BFS-2.36/4.75/9.5	35.6%
BFS-2.36/4.75/9.5	35.0%

$$porosity = 36.52\alpha + 39.62\beta + 43.12\chi - 9.44\alpha\beta - 26.04\alpha\chi - 1.04\beta\chi$$

$$R^2 = 0.99$$

Table 8 Synthetic Lightweight Aggregate theoretical porosity

Blend ID	**Theoretical Aggregate Porosity**
SLA-2.36	38.7%
SLA-4.75	40.5%
SLA-2.36/4.75	35.2%
SLA-2.36/4.75	34.5%
SLA-2.36/4.75	33.6%

$$porosity = 38.7\alpha + 40.5\beta - 20.67\alpha\beta$$

$$R^2 = 0.96$$

Note: SLA aggregate maximum aggregate size is less than 9.5 mm, thus eliminating the 9.5 mm factor.

Table 9 Recycled Concrete Aggregate theoretical porosity

Blend ID	Theoretical Aggregate Porosity
RCA-2.36	42.4%
RCA-4.75	43.4%
RCA-9.5	44.7%
RCA-2.36/4.75	37.9%
RCA-2.36/9.5	39.2%
RCA-4.75/9.5	41.8%
RCA-2.36/4.75/9.5	36.4%
RCA-2.36/4.75/9.5	36.1%
RCA-2.36/4.75/9.5	35.6%

$$porosity = 42.4\alpha + 43.4\beta + 44.7\chi - 20\alpha\beta - 17.4\alpha\chi - 9\beta\chi - 62.4\alpha\beta\chi$$

$$R^2 = 0.99$$

Concrete Porosity Verification by Image Analysis

In Table 10, the Blue Rock aggregate estimated concrete porosity is compared to the image analysis concrete porosity with nine percent concrete paste by volume.

Table 10 Blue Rock Aggregate difference between the estimated concrete porosity and image analysis porosity with nine percent cement paste

Blend ID	Theoretical Aggregate Porosity	Estimated Concrete Porosity	Image Analysis Concrete Porosity
BR-2.36	41.5%	32.5%	38.84%
BR-4.75	42.3%	33.3%	33.68%
BR-9.5	43.7%	34.7%	40.79%
BR-2.36/4.75	36.5%	27.5%	29.40%
BR-2.36/9.5	40.6%	31.6%	34.25%
BR-4.75/9.5	39.9%	30.9%	35.19%
BR-2.36/4.75/9.5	39.1%	30.1%	32.39%
BR-2.36/4.75/9.5	37.7%	28.7%	33.57%
BR-2.36/4.75/9.5	41.5%	32.5%	23.10%

It was estimated with 95 percent confidence that the difference between the Blue Rock estimated concrete porosity and the image analysis concrete porosity with 9 percent concrete paste by volume falls within the interval from -5.51 to 0.59. Since zero is within the interval, there is insufficient evidence to conclude there is a difference between the means.

In Table 11, the Blue Rock aggregate estimated concrete porosity was compared to the image analysis concrete porosity with 18 percent concrete paste by volume.

Table 11 Blue Rock Aggregate difference between the estimated concrete porosity and image analysis porosity with 18 percent cement paste

Blend ID	Theoretical Aggregate Porosity	Estimated Concrete Porosity	Image Analysis Concrete Porosity
BR-2.36	41.5%	23.5%	33.24%
BR-4.75	42.3%	24.3%	37.27%
BR-9.5	43.7%	25.7%	32.67%

BR-2.36/4.75	36.5%	18.5%	26.99%
BR-2.36/9.5	40.6%	22.6%	25.33%
BR-4.75/9.5	39.9%	21.9%	27.48%
BR-2.36/4.75/9.5	39.1%	21.1%	19.55%
BR-2.36/4.75/9.5	37.7%	19.7%	15.74%
BR-2.36/4.75/9.5	41.5%	20.8%	14.60%

It was estimated with 95 percent confidence that the difference between the Blue Rock estimated concrete porosity and the image analysis concrete porosity with 18 percent concrete paste by volume falls within the interval from -8.91 to 1.18. Since zero was within the interval, there was insufficient evidence to conclude there was a difference between the means.

In Table 12 and Table 13, the estimated concrete porosity was compared to the image analysis concrete porosity for 10 and 15 percent cement paste, respectively.

Table 12 Newmarket Aggregate difference between the estimated concrete porosity and image analysis porosity with 10 percent cement paste

Blend ID	**Theoretical Aggregate Porosity**	**Estimated Concrete Porosity**	**Image Analysis Concrete Porosity**
NM-2.36	30.6%	20.6%	21.4%
NM-4.75	34.5%	24.5%	23.6%
NM-9.5	36.3%	26.3%	27.8%
NM-2.36/4.75	32.9%	22.9%	21.3%
NM-2.36/9.5	34.0%	24.0%	23.9%
NM-4.75/9.5	34.0%	24.0%	25.6%
NM-2.36/4.75/9.5	32.9%	22.9%	22.9%
NM-2.36/4.75/9.5	32.4%	22.4%	22.8%
NM-2.36/4.75/9.5	32.2%	22.2%	22.7%

It was estimated with 95 percent confidence that the difference between the Newmarket estimated concrete porosity and the image analysis concrete porosity with 10 percent cement paste by volume falls within the interval from -1.05 to 0.56. Since zero was within the interval, there was insufficient evidence to conclude there is a difference between the means.

Table 13 Newmarket Aggregate difference between the estimated concrete porosity and image analysis porosity with 15 percent cement paste

Blend ID	Theoretical Aggregate Porosity	Estimated Concrete Porosity	Image Analysis Concrete Porosity
NM-2.36	30.6%	15.6%	16.1%
NM-4.75	34.5%	19.5%	20.5%
NM-9.5	36.3%	21.3%	20.4%
NM-2.36/4.75	32.9%	17.9%	18.2%
NM-2.36/9.5	34.0%	19.0%	19.5%
NM-4.75/9.5	34.0%	19.0%	20.1%
NM-2.36/4.75/9.5	32.9%	17.9%	18.0%
NM-2.36/4.75/9.5	32.4%	17.4%	17.9%
NM-2.36/4.75/9.5	32.2%	17.2%	18.1%

It was estimated with 95 percent confidence that the difference between the Newmarket estimated concrete porosity and the image analysis concrete porosity with 15

percent cement paste by volume falls within the interval from -0.91 to 0.02. Since zero was within the interval, there was insufficient evidence to conclude there was a difference between the means.

Based on the information above the ability to predict concrete porosity from a given aggregates mixture equation and a desired cement paste content was shown to be achievable. The control aggregates, which are on either end of the shape spectrum, verified this through image analysis. This procedure is a crucial step in developing porous concrete pavements, which require a porosity range between 15 percent and 25 percent.

Acoustic Impedance Tube Properties

To ensure the results obtained from the UNH sound impedance were comparable to the Purdue University equipment as required in ASTM standard, six samples were selected to be tested by each impedance tube. In Table 14, the mixture sample identification along with the description is presented. In Figures 27 through 32 the absorption coefficient for a range of frequencies is compared for the UNH and Purdue impedance tubes.

Table 14 Mixture sample identification and descriptions

Mixture Sample Identification	Description
4.75BR10	100 percent 4.75 mm Blue Rock Aggregate with 10 percent cement paste, 100 mm diameter, 200 mm long
4.75NEW10	100 percent 4.75 mm Newmarket Aggregate with 10 percent cement paste, 100 mm diameter, 200 mm long
4.75BFS10	100 percent 4.75 mm Blast Furnace Slag Aggregate with 10 percent cement paste, 100 mm diameter, 200 mm long
4.75SLA10	100 percent 4.75 mm Synthetic Light Weight Aggregate with 10 percent cement paste, 100 mm diameter, 200 mm long

4.75RCA10	100 percent 4.75 mm Recycled Concrete Aggregate with 10 percent cement paste, 100 mm diameter, 200 mm long
75mm2.36BFS/125mm4.75BFS10	2.36 mm Blast Furnace Slag with 10 percent cement paste, 75 mm thick on top of 4.75 mm Blast Furnace Slag with 10 percent cement paste, 125 mm thick, 100 mm diameter

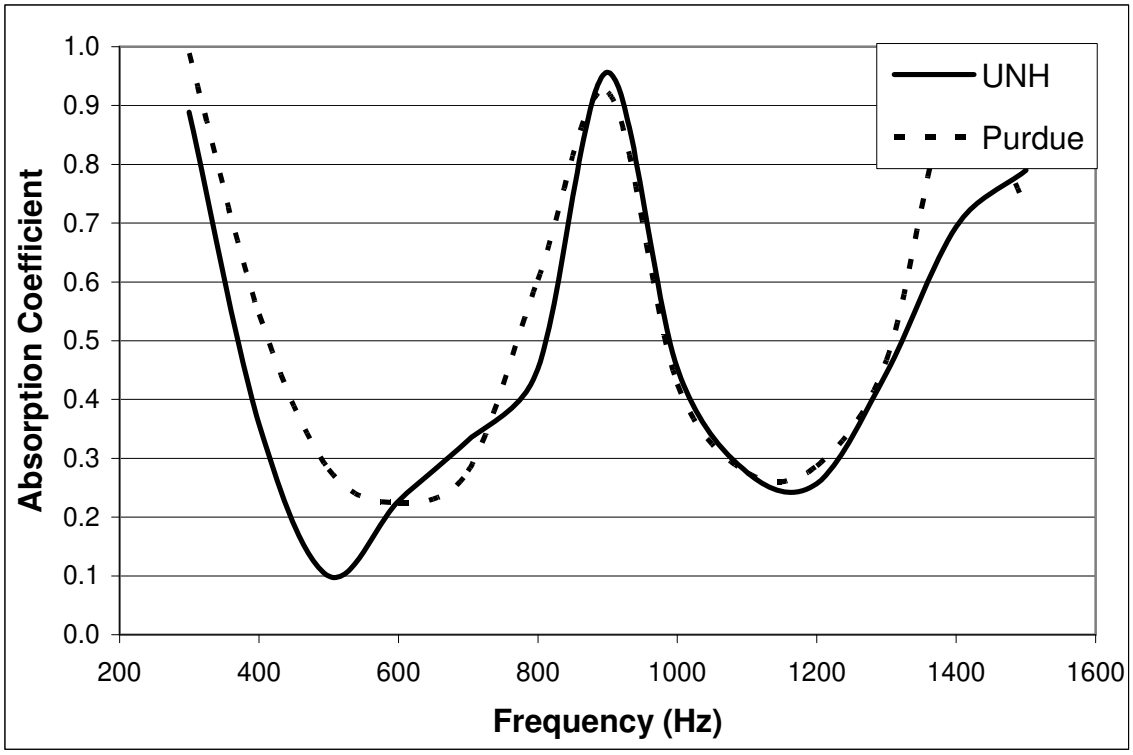

Figure 27 Absorption coefficient versus frequency for UNH and Purdue's impedance tube for sample 4.75BR10

It was estimated with 95 percent confidence that the difference between the UNH and Purdue University absorption coefficient for a given frequency for Sample 4.75BR10 falls within the interval from -0.12 to 0.01. Since zero was within the interval, there was insufficient evidence to conclude there was a difference between the means.

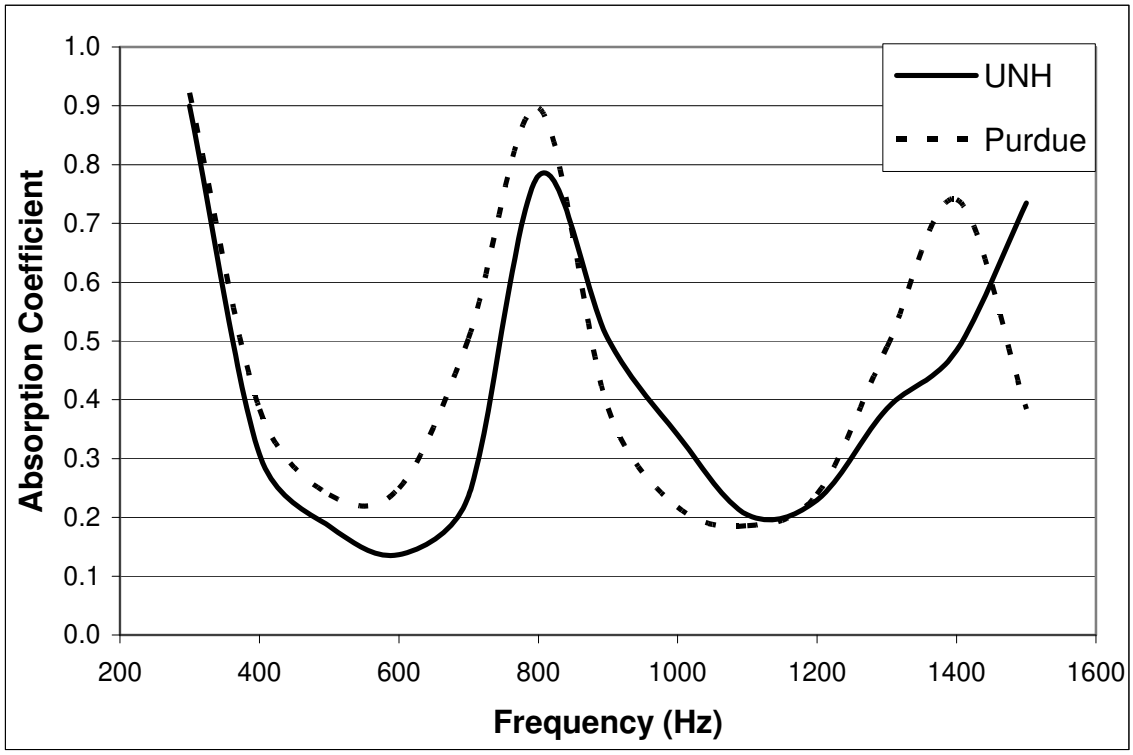

Figure 28 Absorption coefficient versus frequency for UNH and Purdue's impedance tube for sample 4.75NEW10

It was estimated with 95 percent confidence that the difference between the UNH and Purdue University absorption coefficient for a given frequency for Sample 4.75NEW10 falls within the interval from -0.13 to 0.07. Since zero was within the interval, there was insufficient evidence to conclude there was a difference between the means.

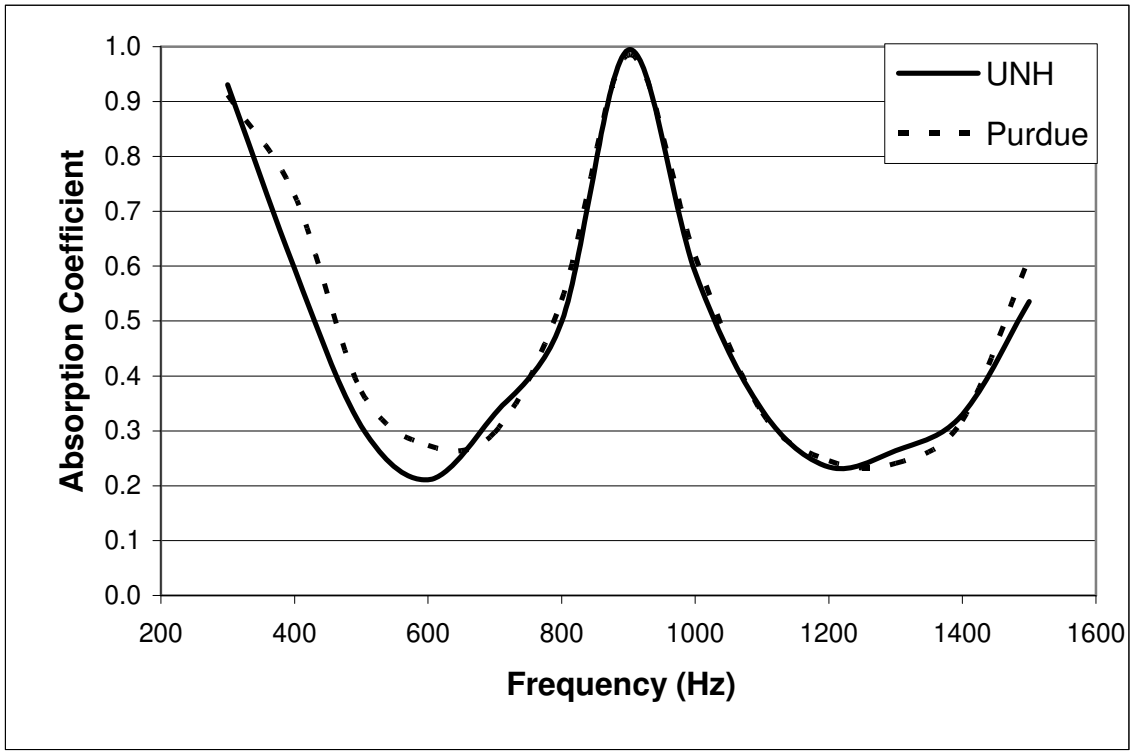

Figure 29 Absorption coefficient versus frequency for UNH and Purdue's impedance tube for sample 4.75BFS10

It was estimated with 95 percent confidence that the difference between the UNH and Purdue University absorption coefficient for a given frequency for Sample 4.75BFS10 falls within the interval from -0.05 to 0.01. Since zero was within the interval, there was insufficient evidence to conclude there was a difference between the means.

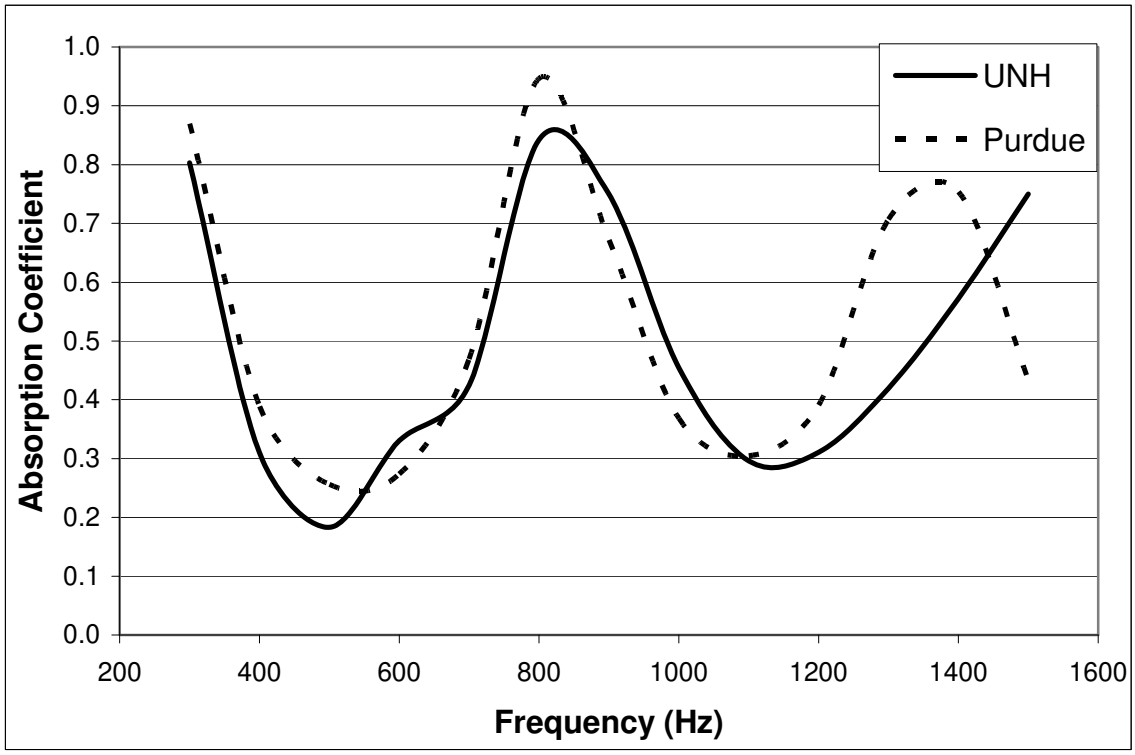

Figure 30 Absorption coefficient versus frequency for UNH and Purdue's impedance tube for sample 4.75SLA10

It was estimated with 95 percent confidence that the difference between the UNH and Purdue University absorption coefficient for a given frequency for Sample 4.75SLA10 falls within the interval from -0.12 to 0.06. Since zero was within the interval, there was insufficient evidence to conclude there was a difference between the means.

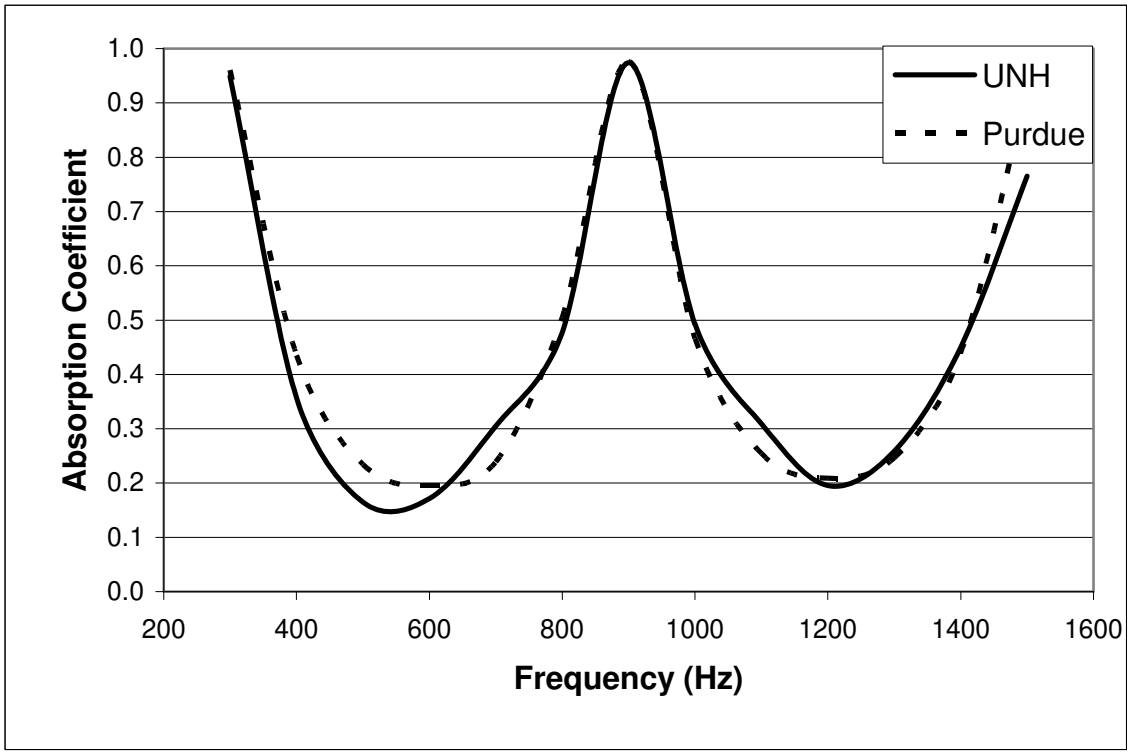

Figure 31 Absorption coefficient versus frequency for UNH and Purdue's impedance tube for sample 4.75RCA10

It was estimated with 95 percent confidence that the difference between the UNH and Purdue University absorption coefficient for a given frequency for Sample 4.75RCA10 falls within the interval from -0.05 to 0.02. Since zero was within the interval, there was insufficient evidence to conclude there was a difference between the means.

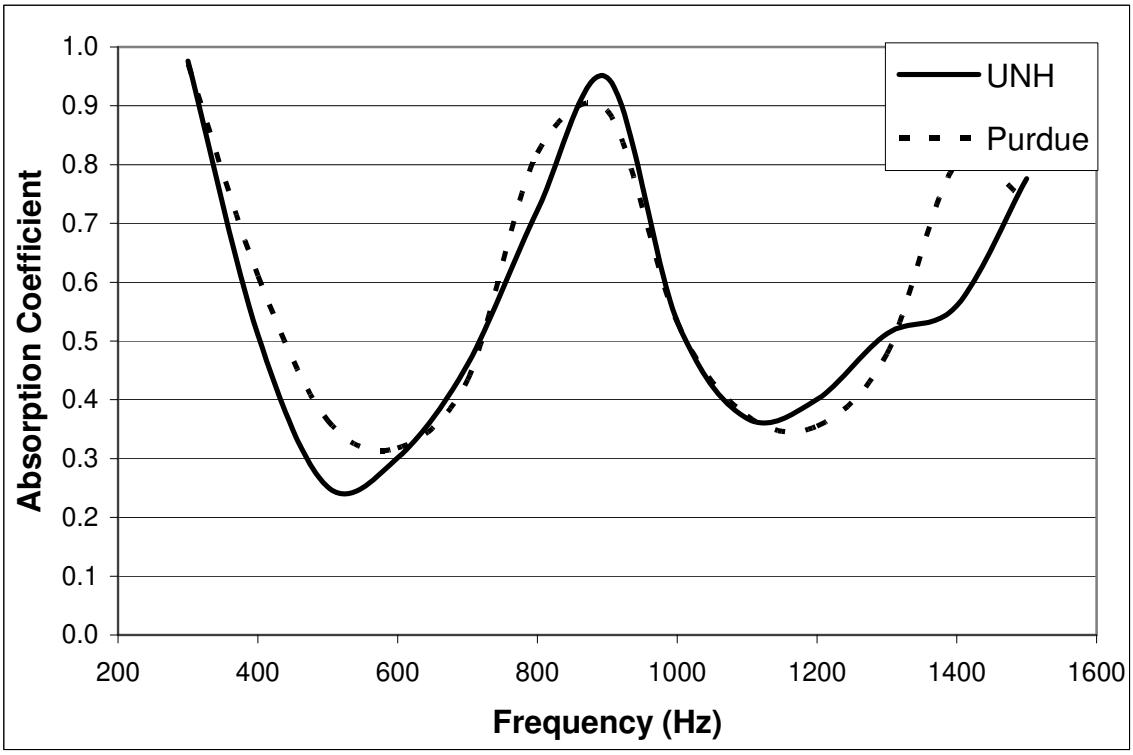

Figure 32 Absorption coefficient versus frequency for UNH and Purdue's impedance tube for sample 75mm2.36BFS/125mm4.75BFS10

It was estimated with 95 percent confidence that the difference between the UNH and Purdue University absorption coefficient for a given frequency for Sample 75mm2.36BFS/125mm4.75BFS10 falls within the interval from -0.08 to 0.02. Since zero was within the interval, there was insufficient evidence to conclude there was a difference between the means.

The results presented above are significant in that the UNH sound impedance tube is able to quantify the absorption coefficient. The UNH setup exceeded the expectations set forth at the beginning of the research. It was only expected to compare sample to sample, thus allowing the samples to be ranked in order from most absorptive to least

absorptive. As shown in Figure 27 there are some points that do not seem to fit the rest of the data, which is most likely due to human error and/or background noise in the lab. At approximately 500 Hz the UNH results do not fit the expected profile of the data. A frequency filter was used and all unnecessary electrical equipment was turned off, however stray signals may not have been eliminated from the testing. Ideally the UNH data should have been collected in an insulated room free from any interference, however such was not available. Another significant finding in the results is that the peak absorption occurs nearly at the same frequency for both setups.

Once the UNH impedance tube method was shown to be comparable to the Purdue setup, the variables that affect absorption and frequencies at which the peak absorption occurs were examined. The first variable examined was modulus of elasticity of the aggregate. Figures 33 and 34 show the absorption coefficient for a range of frequencies for plastic, glass, and steel 12.5 mm balls used as aggregate with 7 percent and 12 percent paste, respectively.

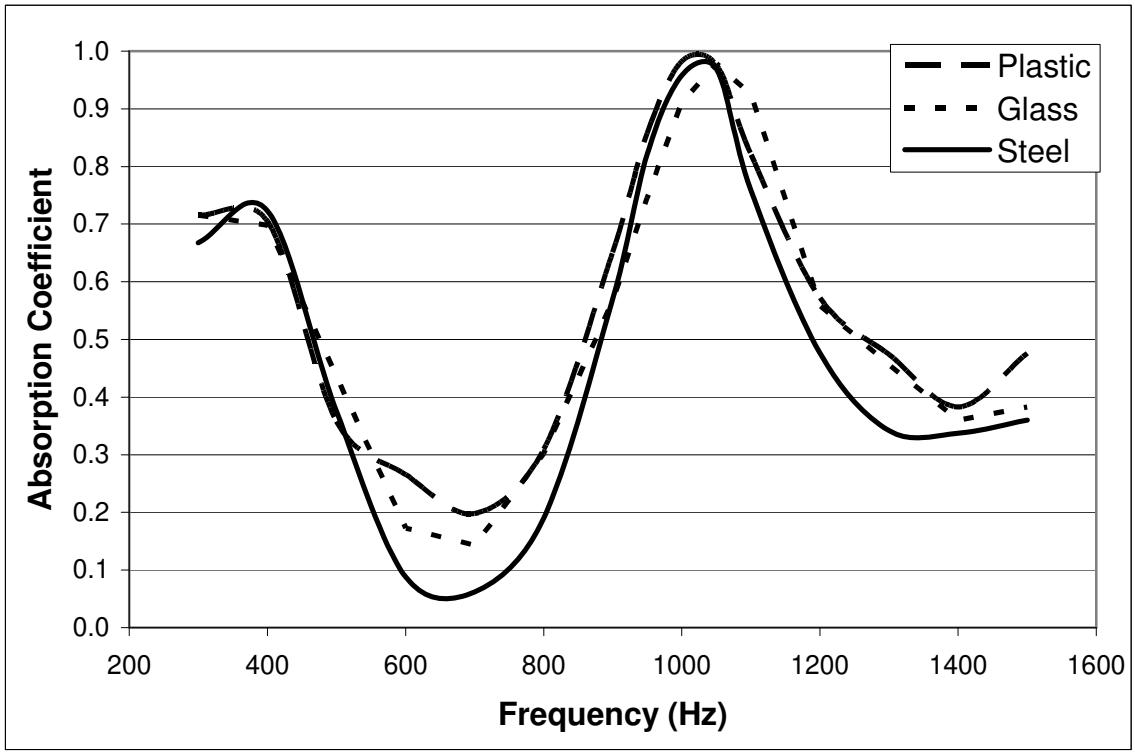

Figure 33 Comparing modulus of elasticity of plastic, glass, and steel 12.5 mm with 7 percent cement paste

Using matched pair analysis the plastic was compared to the glass, giving a 95 percent confidence interval of -0.01 to 0.06. Since zero was within the interval, there was insufficient evidence to conclude there was a difference between the means. When steel was compared to plastic and glass the 95 percent confidence intervals were 0.04 to 0.10 and 0.01 to 0.08, respectively.

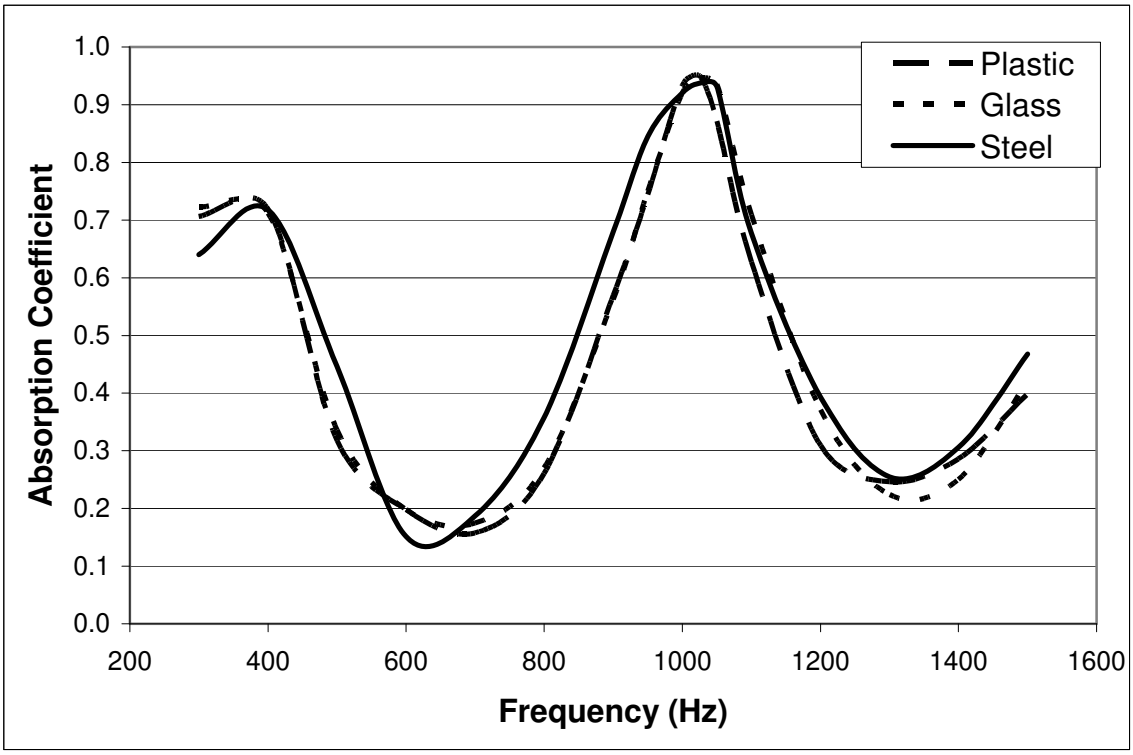

Figure 34 Comparing modulus of elasticity of plastic, glass, and steel 12.5 mm with 12 percent cement paste

Using matched pair analysis the plastic when compared to the glass, the 95 percent confidence interval was -0.03 to 0.01. Since zero is within the interval, there was insufficient evidence to conclude there was a difference between the means. However, when steel was compared to plastic and glass the 95 percent confidence intervals were -0.07 to -0.02 and -0.06 to -0.01, respectively. As expected there was a difference between steel and plastic and glass at both 7 percent and 12 percent cement paste, however it is not likely to have an aggregate modulus higher than 100 GPa. It was anticipated that if the aggregate modulus of elasticity was comparable to that of portland cement concrete then it most likely would not be a variable that would affect absorption

properties. The steel aggregate is changing the modulus of elasticity of the entire sample, therefore also changing the sound absorbing capabilities of the sample. If the modulus of elasticity of the sample is significantly changed, the sound absorbing capabilities will also change.

Different samples depths are presented in Figure 35 through Figure 37 for 100 percent 4.75 mm Blue Rock aggregate with 10 percent cement paste.

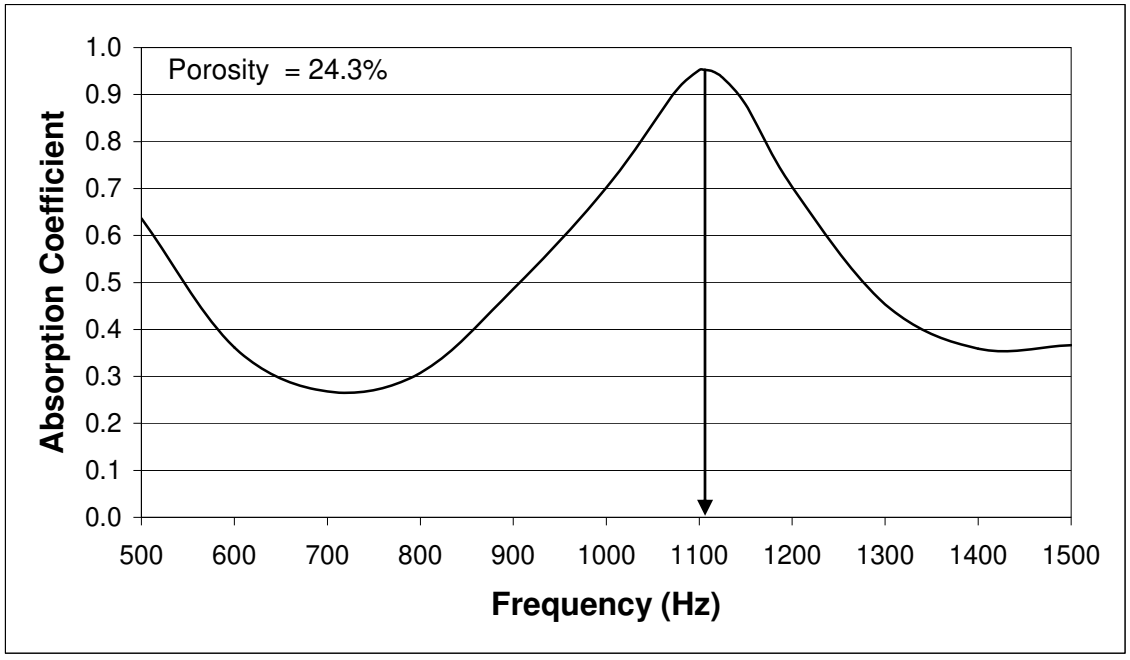

Figure 35 4.75 mm Blue Rock Aggregate 100 percent with 10 percent cement paste, 150 mm long

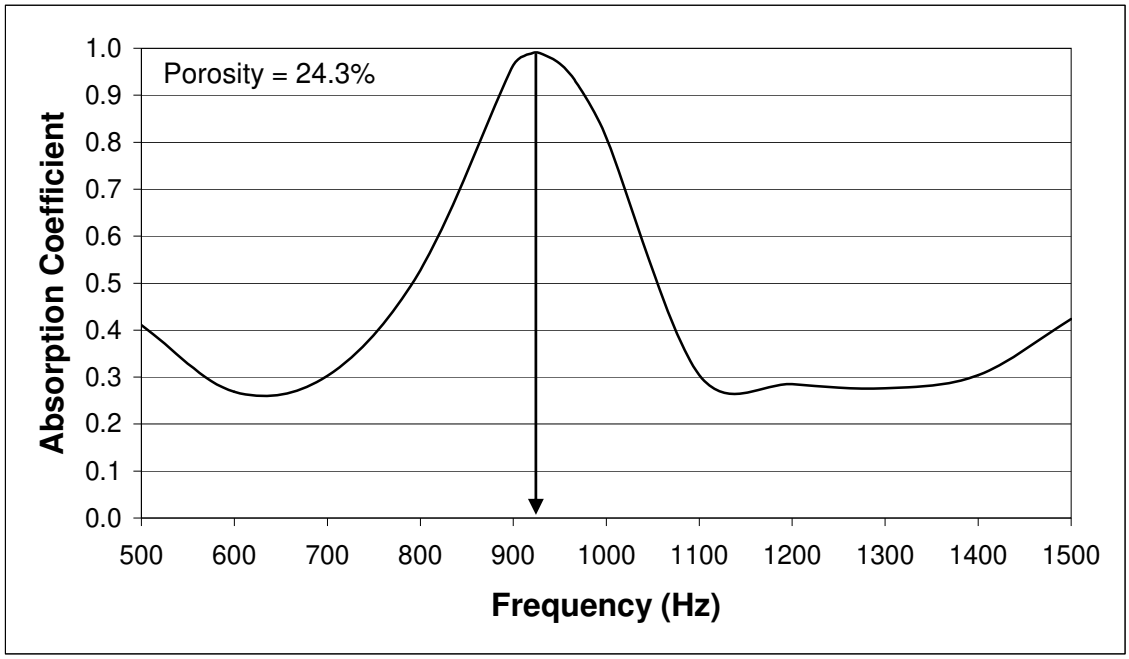

Figure 36 4.75 mm Blue Rock Aggregate 100 percent with 10 percent cement paste, 175 mm long

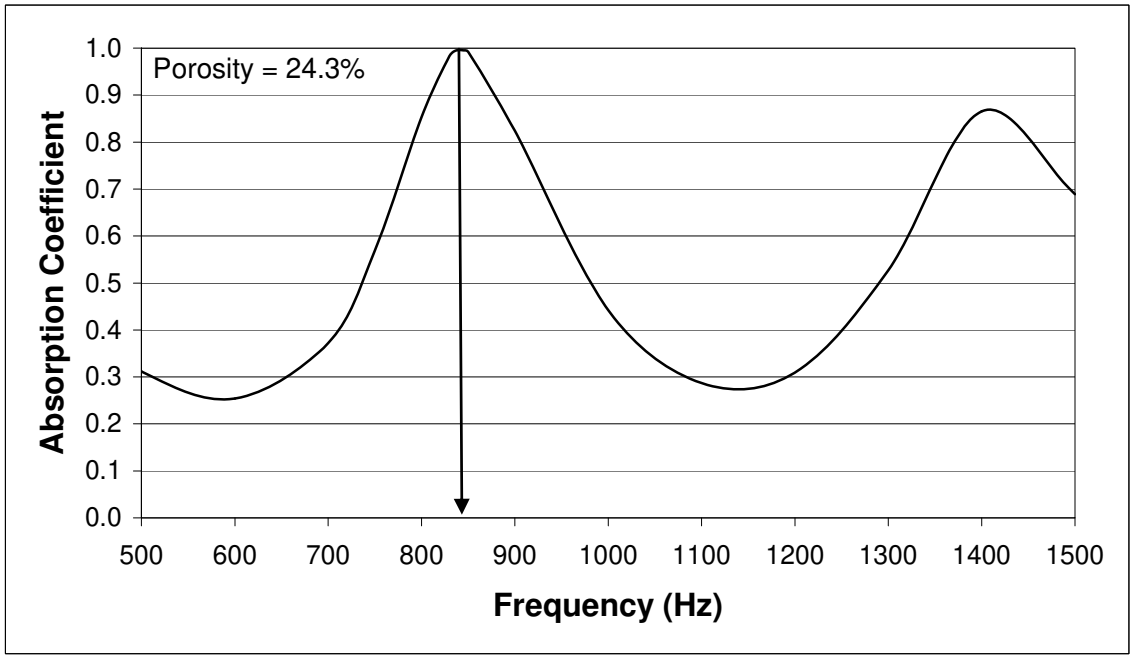

Figure 37 4.75 mm Blue Rock Aggregate 100 percent with 10 percent cement paste, 200 mm long

It appears that as the depth increases the position of the peak absorption occurs at a lower frequency, which as shown in Figure 38.

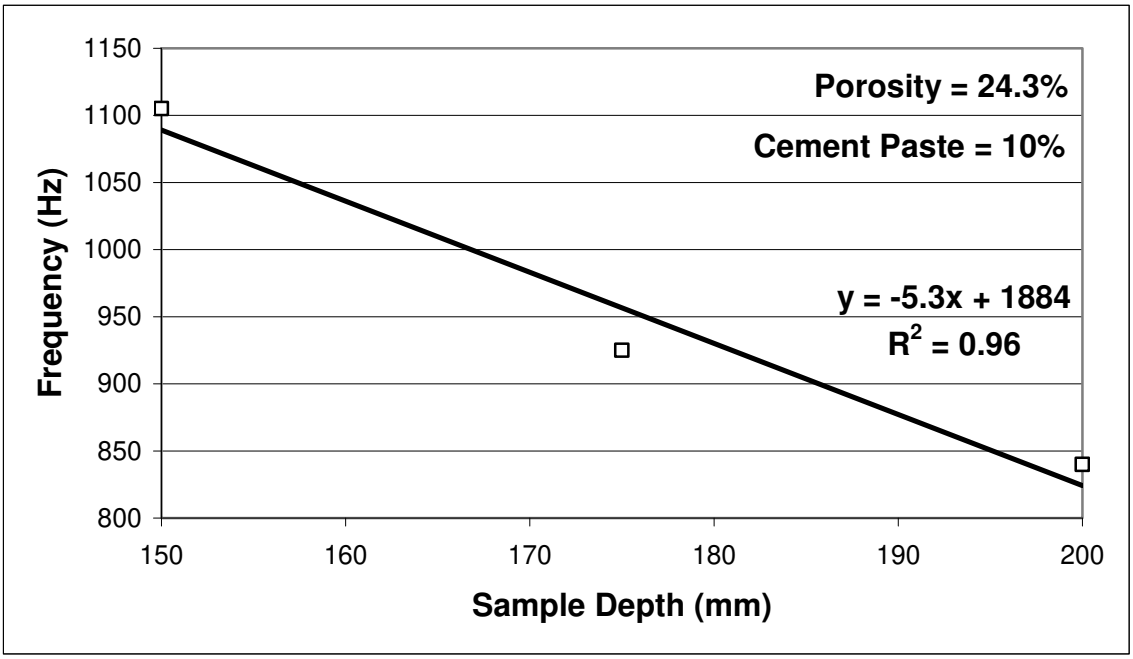

Figure 38 Frequency at peak absorption versus sample depth

Different samples depths are presented in Figure 39 through Figure 42 for 100 percent 4.75 mm Newmarket aggregate with 10 percent cement paste.

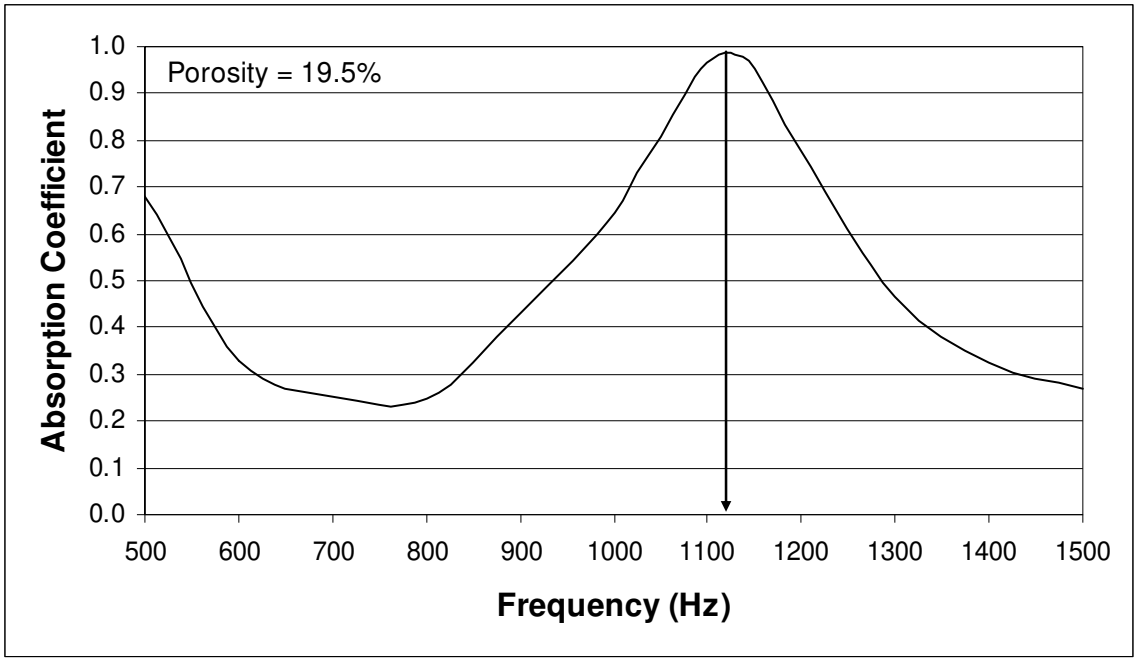

Figure 39 4.75 mm Newmarket Aggregate 100 percent with 10 percent cement paste, 150 mm long

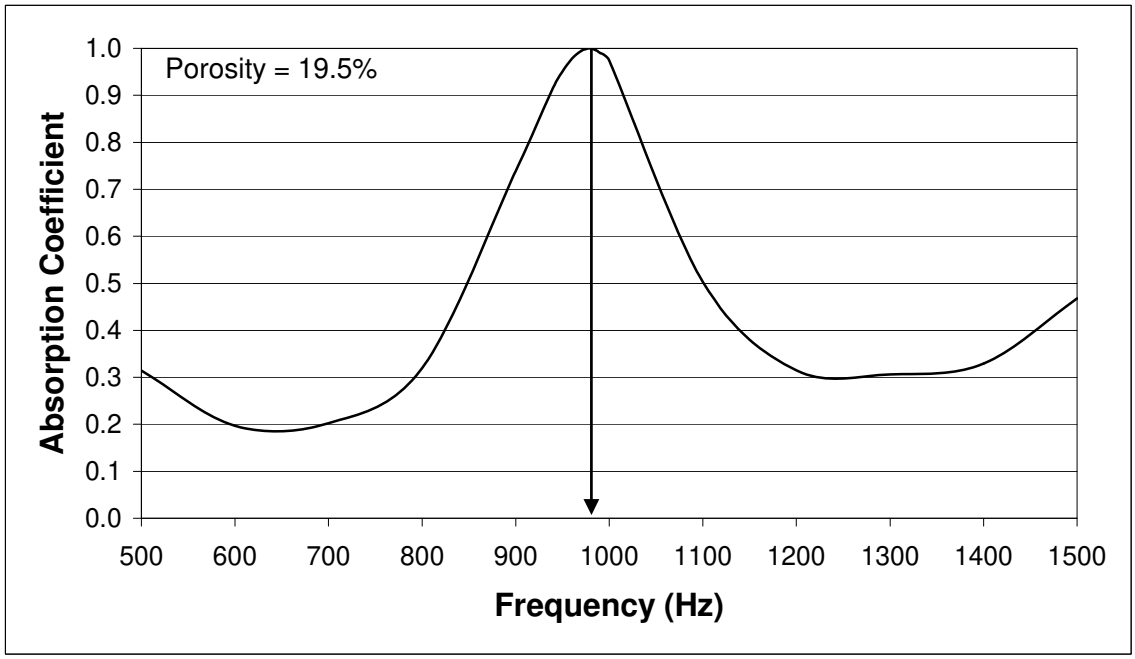

Figure 40 4.75 mm Newmarket Aggregate 100 percent with 10 percent cement paste, 175 mm long

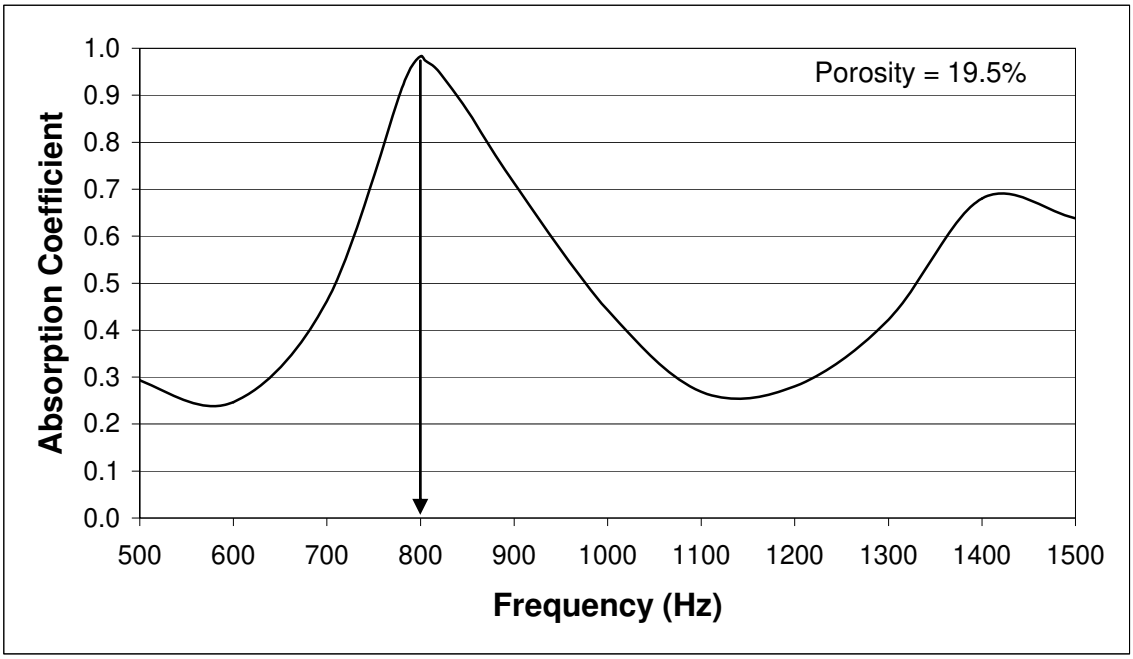

Figure 41 4.75 mm Newmarket Aggregate 100 percent with 10 percent cement paste, 200 mm long

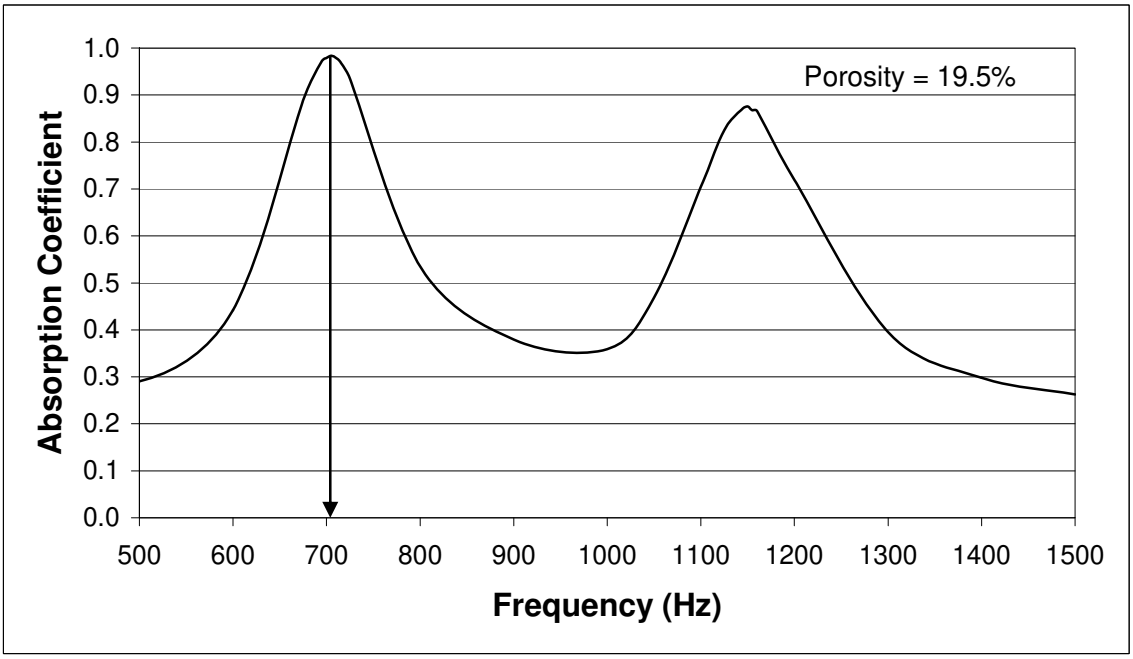

Figure 42 4.75 mm Newmarket Aggregate 100 percent with 10 percent cement Paste, 250 mm long

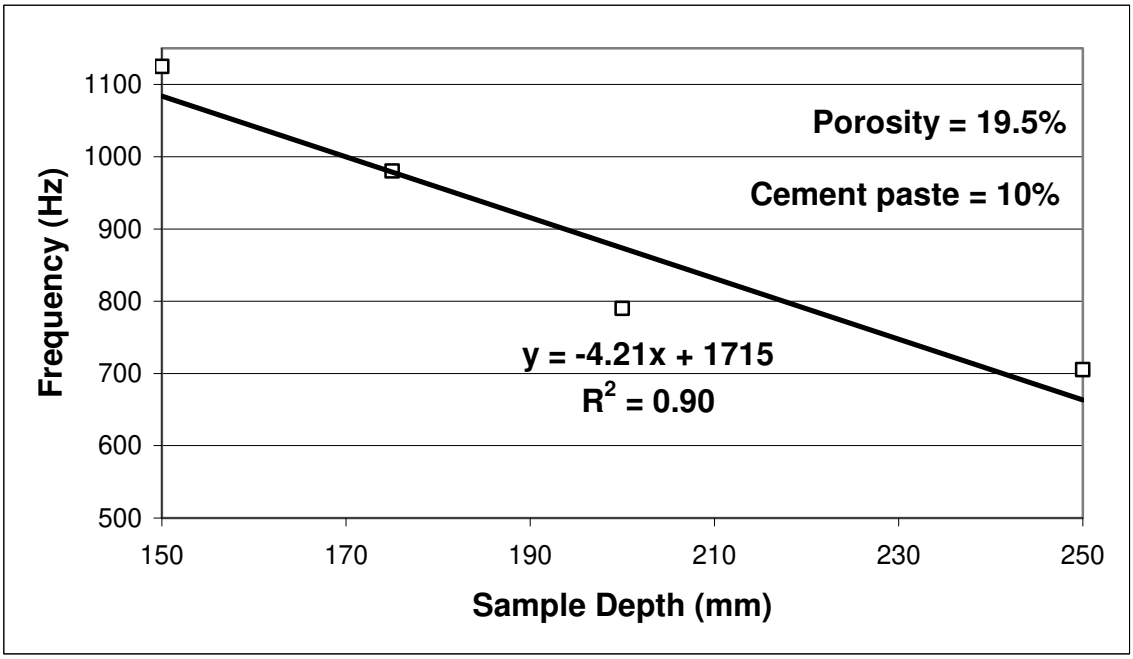

Figure 43 Frequency at peak absorption versus sample depth

Figures 44 through 47, show frequency as a function of sample depth for two layer samples. The upper layer was 100 percent 2.36 SLA, while the bottom layer was 100 percent BFS both with 10 percent cement paste. The depths were varied to determine its affect on the absorption coefficient and corresponding frequency. In Figure 48, the frequency at which the peak absorption coefficient occurs is plotted against the upper layer thickness, while in Figure 49 the peak absorption coefficient is plotted against the upper layer thickness.

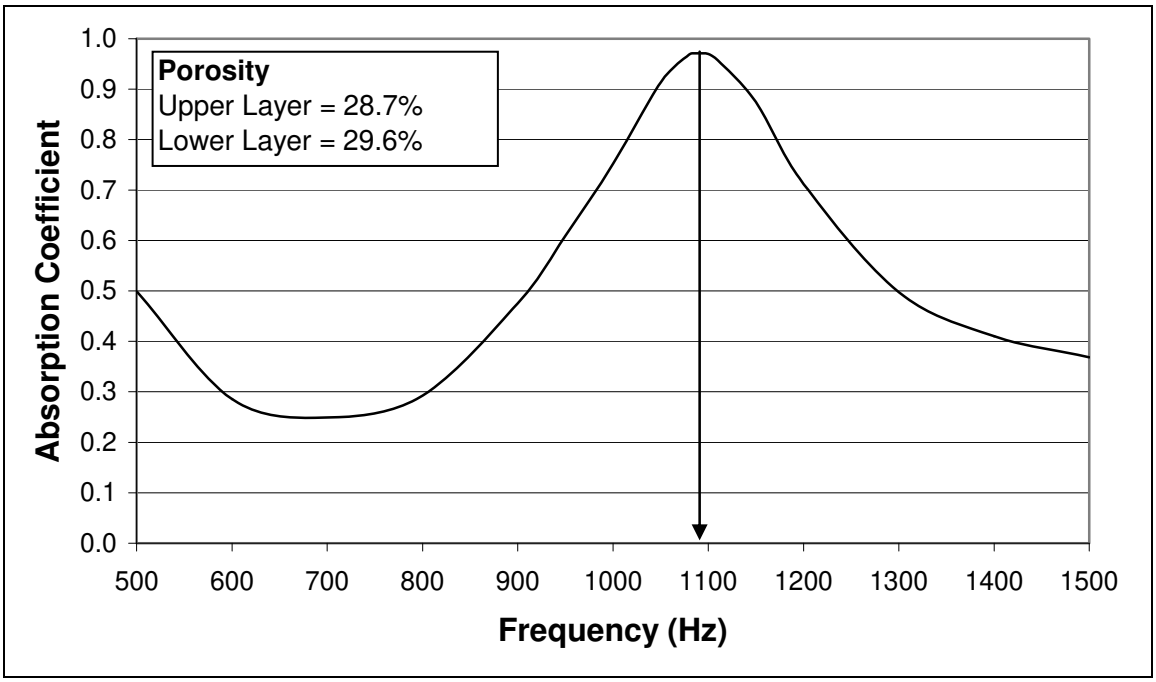

Figure 44 25 mm 2.36 mm SLA 100 percent on 150 mm 4.75 BFS 100 percent with 10 percent cement paste, 75 mm long

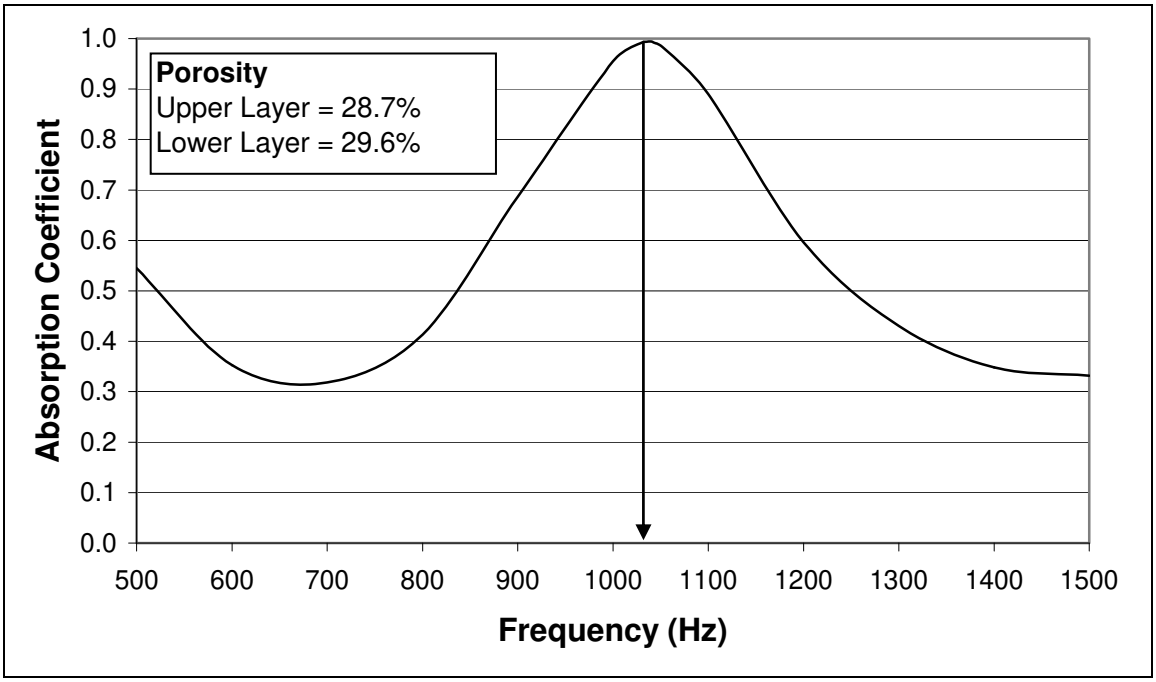

Figure 45 50 mm 2.36 mm SLA 100 percent on 125 mm 4.75 BFS 100 percent with 10 percent cement paste, 175 mm long

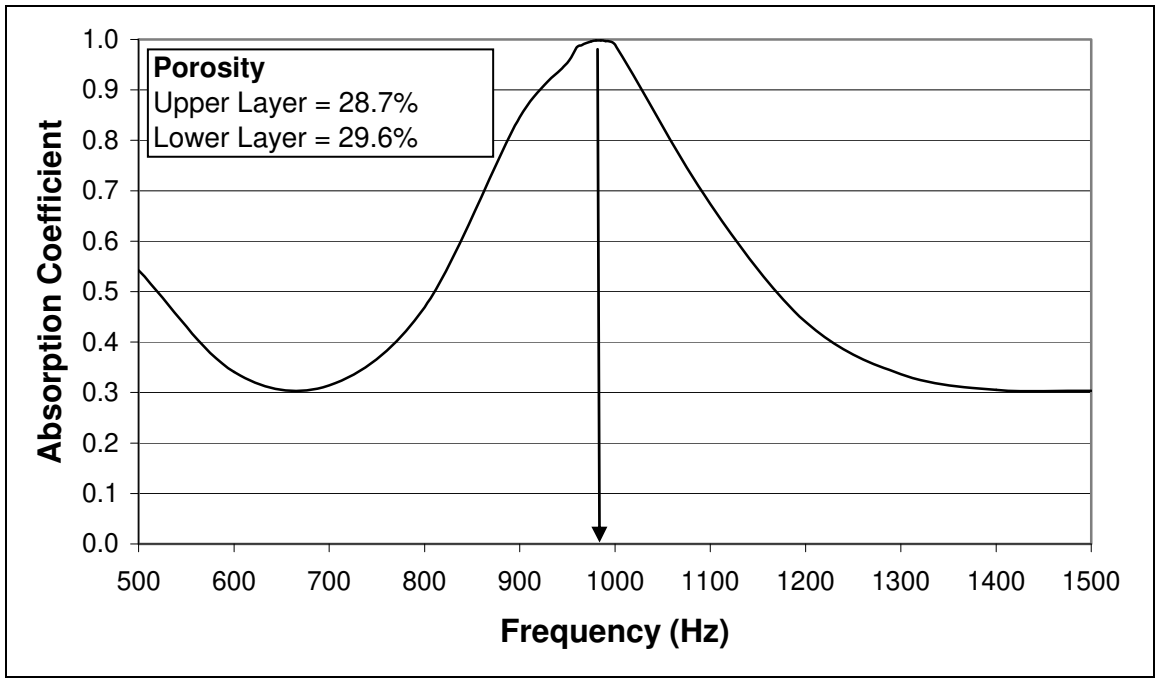

Figure 46 75 mm 2.36 mm SLA 100 percent on 100 mm 4.75 BFS 100 percent with 10 percent cement paste, 175 mm long

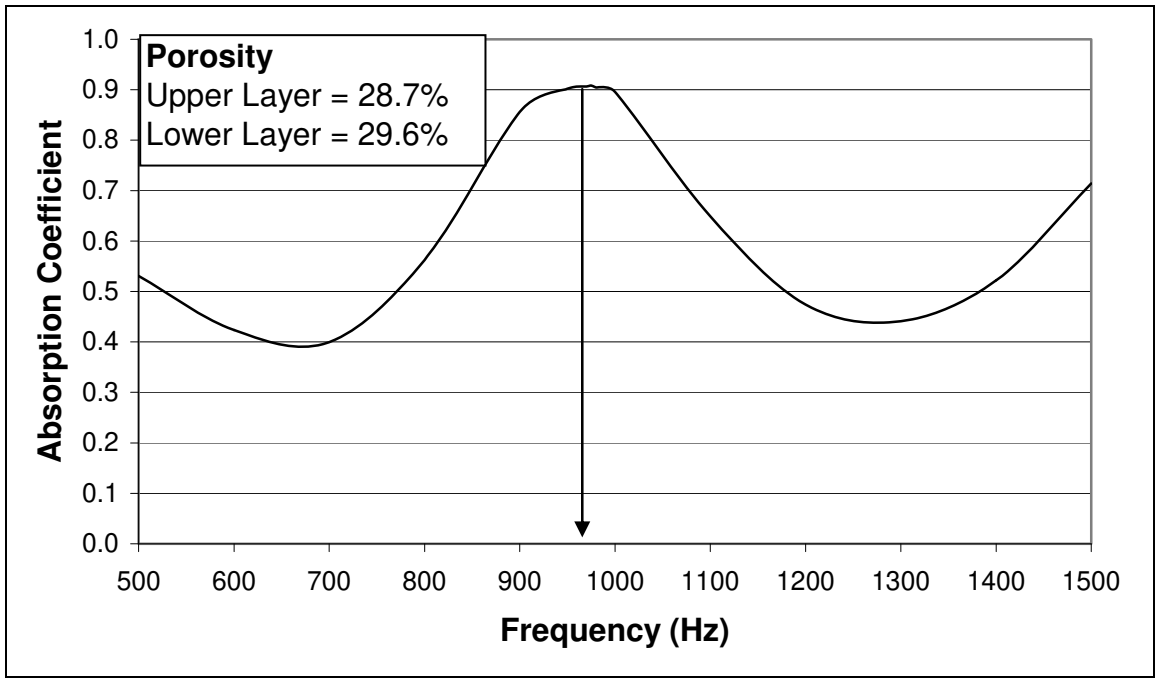

Figure 47 100 mm 2.36 mm SLA 100 percent on 75 mm 4.75 BFS 100 percent with 10 percent cement paste, 175 mm long

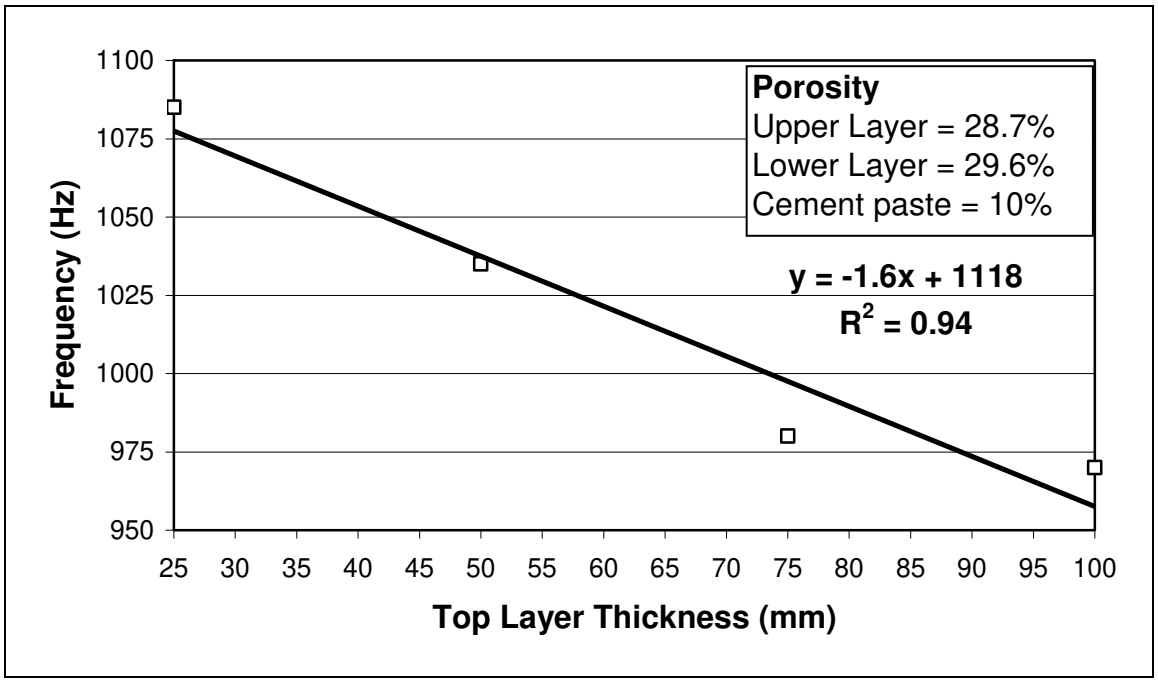

Figure 48 Frequency at peak absorption versus upper layer thickness

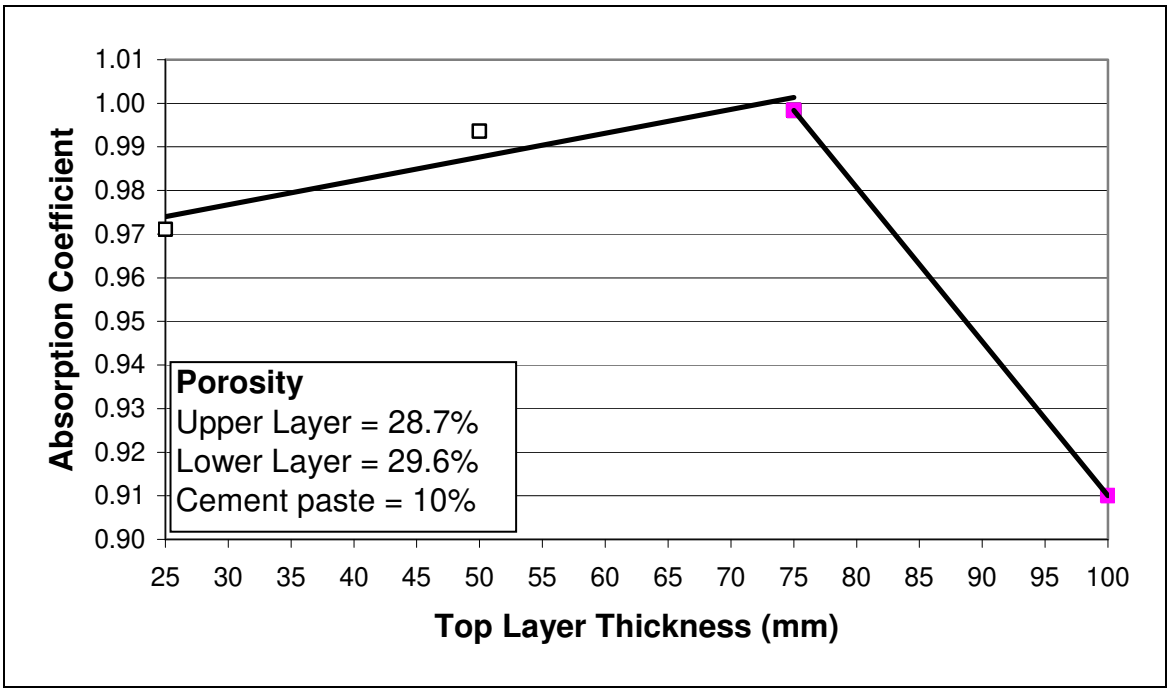

Figure 49 Peak absorption coefficient versus upper layer thickness

For the two-layer samples there appears to be an inverse relationship between with upper layer thickness and frequency at peak absorption. Although, there seems to be point where this phenomena diminishes. Varying upper layer thickness slowly increases the peak absorption coefficient up to a certain point then it rapidly decreases.

From a design viewpoint for the ability to determine these trends is important because once a particular frequency is identified for abatement the maximum absorption coefficient can be immediately identified. For example, if the target frequency to be reduced is between 1,000 and 1,050 Hertz, the upper layer thickness range is easily identified as shown in Figure 50.

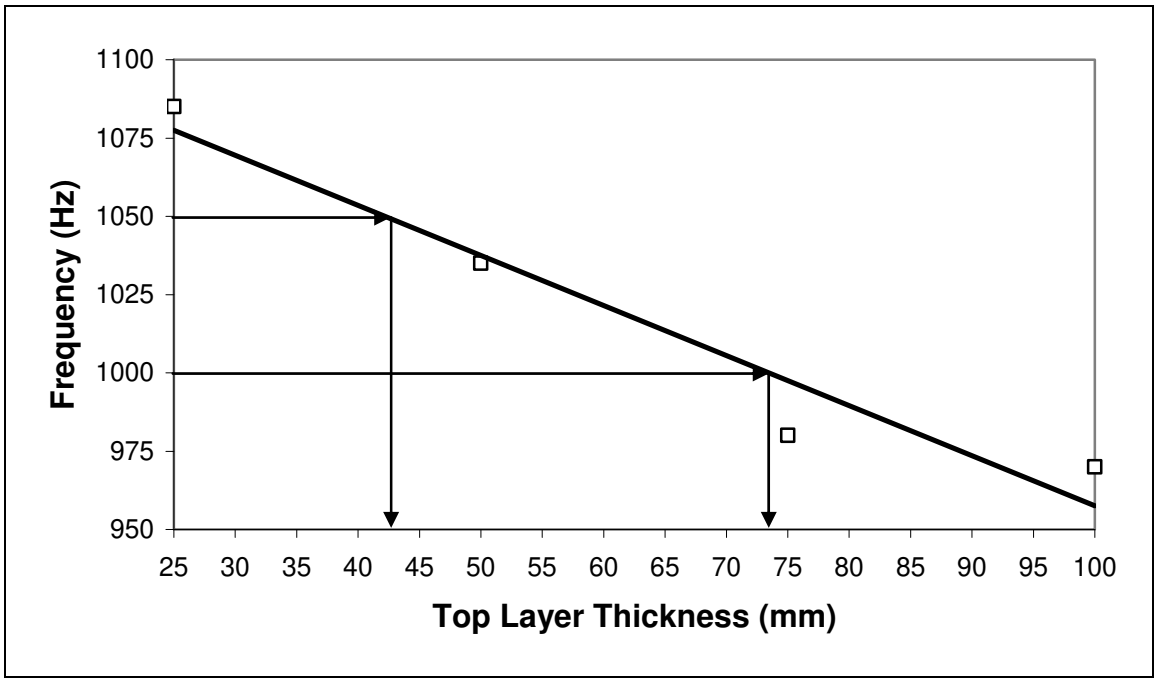

Figure 50 Frequency at peak absorption versus upper layer thickness

The corresponding upper layer thicknesses for the targeted frequency range are between 43 and 73 mm. Using Figure 49 above, the optimum upper layer thickness for this particular case would be approximately 70 mm, which would produce a 0.99 absorption coefficient at 1,000 Hertz. The flexural strength, skid resistance, freeze-thaw resistance, and constructability would have to be examined to ensure all criteria are met before deciding on the best mixture for achieving ideal sound absorbing properties for PCC pavements.

In Table 15, the concrete porosity for a given aggregate is presented along with corresponding values of frequency at peak absorption and the peak absorption coefficient for various samples.

Table 15 Concrete porosity for aggregate source with frequency at peak absorption and peak absorption coefficient for 200 mm samples

Aggregate	Porosity (%)	Frequency at Peak Absorption (Hz)	Peak Absorption Coefficient
Blue Rock	32.3	840	0.9956
Blue Rock	27.3	785	0.9705
Blue Rock	22.3	730	0.9444
Blue Rock	17.3	700	0.9230
Newmarket	29.5	850	0.9929
Newmarket	24.5	800	0.9831
Newmarket	19.5	845	0.9733
Newmarket	14.5	790	0.9635
BFS	29.6	900	0.9900
BFS	24.6	845	0.9710
BFS	19.6	730	0.9540
BFS	14.6	695	0.9310
SLA	30.5	800	0.9400
SLA	25.5	745	0.9310
SLA	20.5	710	0.9220
SLA	15.5	685	0.9150
RCA	33.4	900	0.9700
RCA	28.4	860	0.9480
RCA	23.4	805	0.9210
RCA	18.4	790	0.9000

In Figure 51, the frequency is plotted against the porosity for each given aggregate source.

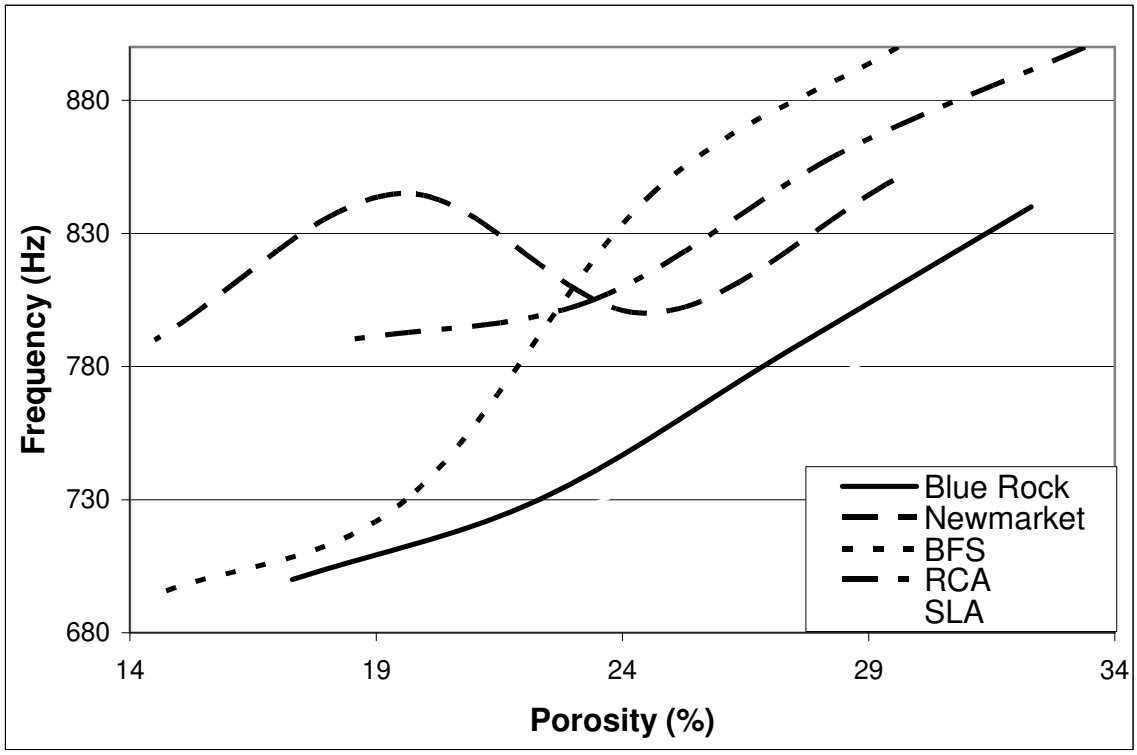

Figure 51 Frequency at peak absorption versus concrete porosity for aggregate source

With the exception of the Newmarket aggregate, the other aggregate sources show similar trends; as the concrete porosity increases the frequency at peak absorption increases. The sample for the Newmarket aggregate that does not follow the trend was reexamined in the impedance tube, and similar results were recorded. Further analysis of the concrete porosity was required; therefore, the sample was cut and polished perpendicular to its vertical axis to determine the porosity throughout the length of the sample. The cut samples were analyzed by image analysis to verify concrete porosity. Table 16 shows the concrete porosity of the sample, which had a predicted average concrete porosity of 19.5 percent.

Table 16 Measured concrete porosity verified within Newmarket Aggregate sample with average predicted average porosity of 19.5 percent

Distance From Top Surface (mm)	**Concrete Porosity By Image Analysis (%)**

0	25.8
25	26.7
50	24.6
75	19.9
100	18.6
125	18.1
150	17.6
175	14.8
200	15.4

These data show the concrete's porosity decreases with depth of the sample. The average concrete porosity throughout the sample is 20.2 percent, near the predicted 19.5 percent, however the cement paste must not have been thoroughly distributed in this sample, most likely resulting from over vibrating the sample causing paste to increase with depth.

In Figure 52, the concrete porosity is plotted against the peak absorption coefficient for each aggregate source to compare sound absorbing capabilities of the various test aggregates.

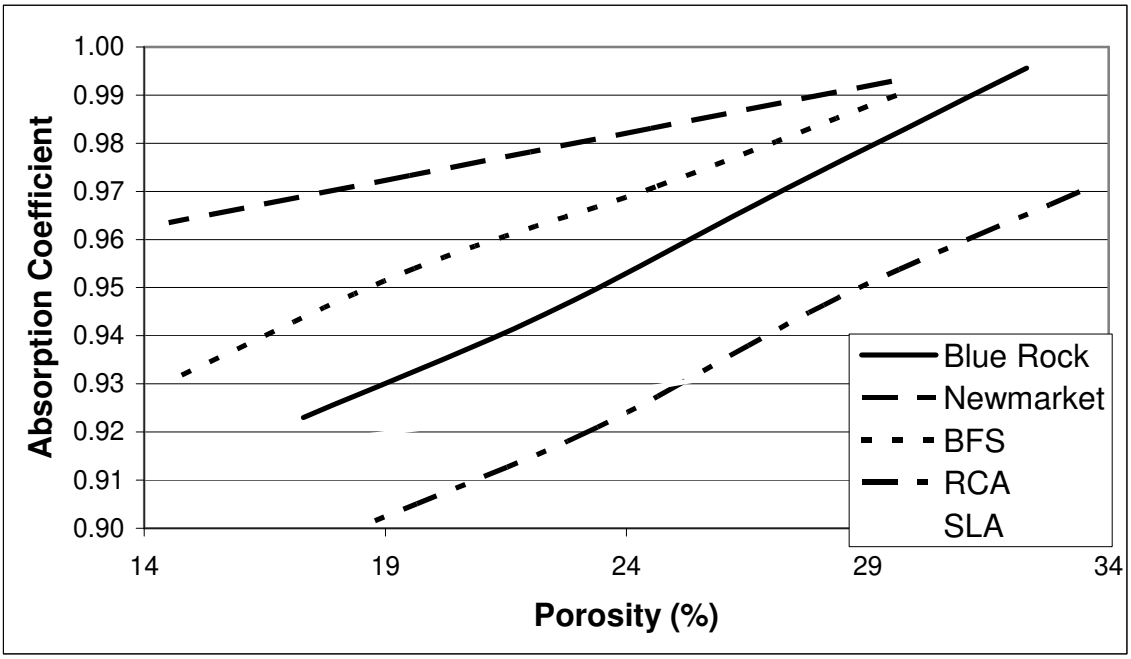

Figure 52 Absorption coefficient versus concrete porosity for aggregate source

Based on these results there is in general no direct relationship between the absorption coefficient and concrete porosity of the various aggregate sources. Within the aggregate sources as porosity increases the absorption coefficient increases, however each aggregate sources seems to have a different rate at which that change occurs. The data also suggests that the rounded type aggregates have better sound absorbing capabilities at a lower concrete porosity. This is consistent with basic matrix analysis, angular aggregates tend to pack better than rounded aggregates, and therefore there may be more interconnected pores in the rounded aggregate blends. This may become important when trying to optimize a mixture design in which flexural strength becomes a factor.

The phenomena seen with the Newmarket sample that affected the frequency at peak absorption does not seem to show up when examining the concrete porosity and the absorption coefficient. This may be because the absorption coefficient only depends on the overall porosity of the sample, however the frequency at which the peak absorption occurs may depend on the interconnectivity of the pores.

Pulse Velocity

In Table 17, the concrete porosity for an aggregate source is compared to the resulting pulse velocity value for a given sample. In Figure 53, the concrete porosity is plotted against the pulse velocity for a given aggregate source.

Table 17 Concrete porosity for aggregate source with pulse velocity

Aggregate	Porosity (%)	Pulse Velocity (m/s)
Blue Rock	32.3	1921
Blue Rock	27.3	2317
Blue Rock	22.3	2601
Blue Rock	17.3	2984
Newmarket	29.5	2244
Newmarket	24.5	2469
Newmarket	19.5	2649
Newmarket	14.5	2822
BFS	29.6	1522
BFS	24.6	2644
BFS	19.6	3105
BFS	14.6	3607
SLA	30.5	858
SLA	25.5	1274
SLA	20.5	1536
SLA	15.5	1869
RCA	33.4	1877
RCA	28.4	2286
RCA	23.4	2605
RCA	18.4	2973

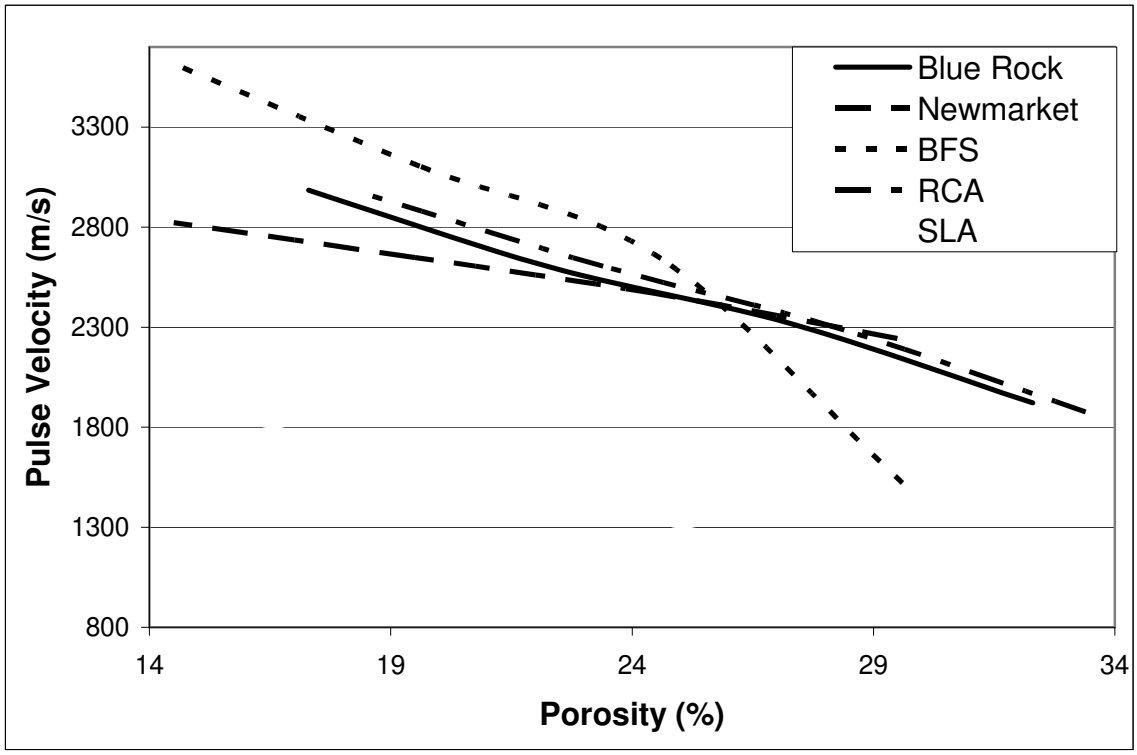

Figure 53 Pulse velocity versus concrete porosity for aggregate source

As shown in Figure 53, the pulse velocity decreases as the concrete porosity increases. With the exception of the BFS aggregate source the rate at which the change occurs is consistent. The reason why the BFS source does not change consistently is that the sample with 29.6 percent concrete porosity had a very irregular surface due to the low cement paste content. This irregular surface prevented the transducers from sitting flat on the concrete surface.

Another difference among the results in Figure 53 is that all aggregate sources seem to be within the same range of pulse velocity for a given concrete porosity with the exception of the SLA aggregate source. With the exception of the SLA, the aggregate sources have similar a modulus to that of concrete. The SLA is composed of fly ash and waste plastic, therefore having a much lower modulus of elasticity than that of the other aggregate sources.

Flexural Strength

In Table 18, concrete porosity is compared to the resulting flexural strength value for a given sample. In Figure 54, the concrete porosity is plotted against the flexural strength for a given aggregate source.

Table 18 Concrete porosity for aggregate source with flexural strength

Aggregate	Porosity (%)	Flexural Strength (MPa)
Blue Rock	32.3	315
Blue Rock	27.3	406
Blue Rock	22.3	539
Blue Rock	17.3	660
Newmarket	29.5	298
Newmarket	24.5	392
Newmarket	19.5	488
Newmarket	14.5	617
BFS	29.6	281
BFS	24.6	345
BFS	19.6	408
BFS	14.6	507
SLA	30.5	277
SLA	25.5	326
SLA	20.5	399
SLA	15.5	487
RCA	33.4	322
RCA	28.4	411
RCA	23.4	538
RCA	18.4	644

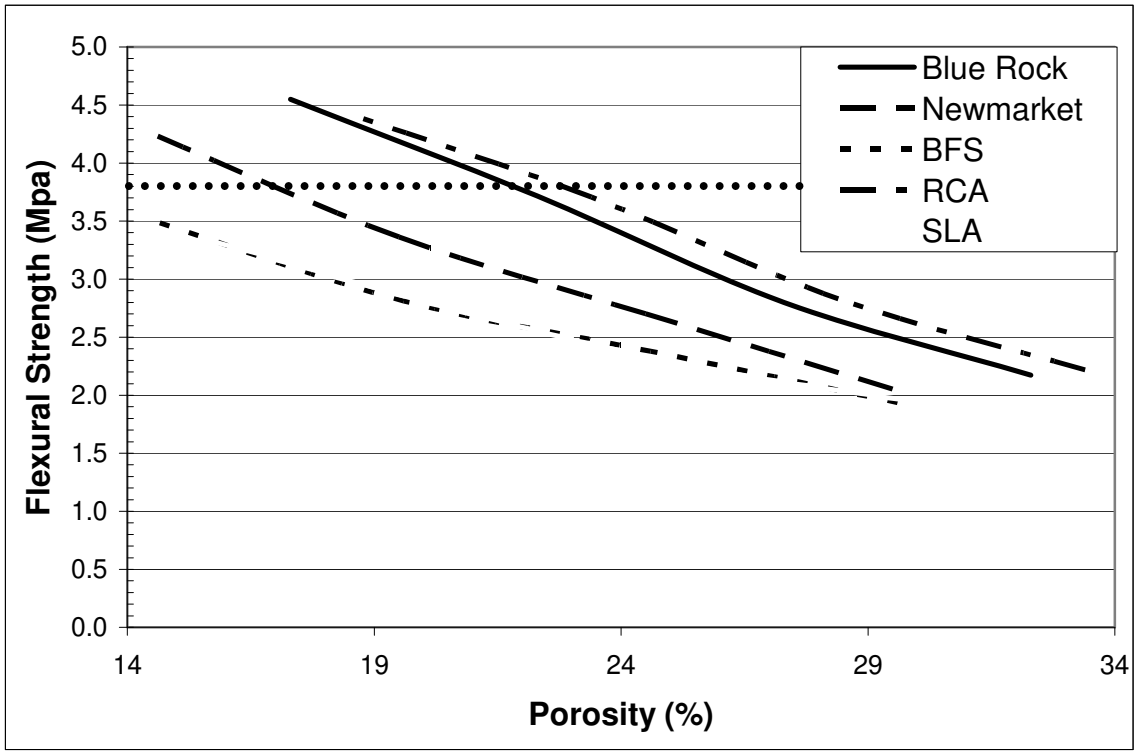

Figure 54 Flexural strength versus concrete porosity for aggregate source

As shown above the trend is similar for all aggregate sources; as porosity increases the flexural strength decreases. The flexural strength appears to be changing at a similar rate for all aggregate sources. As expected the angular aggregates, Blue Rock and RCA, have higher flexural strengths at a given porosity compared to that of the rounded aggregates, Newmarket and BFS. The higher flexural strength of the angular aggregates is likely due to the ability to mesh together as well as a better bond with the angular surfaces.

The dotted line in the figure represents the minimum flexural strength, 3.8 MPa, for PCC pavements, suggested in previous sections. The conventional aggregates meet the desired porosity of 20 percent, however the recycled aggregates will need further investigation in this area to achieve the required minimum flexural strength at the preferred 20 percent porosity.

Compressive Strength

Concrete porosity is compared to the resulting compressive strength for a given sample as shown in Table 19. In Figure 55, the compressive strength is plotted against the concrete porosity for a given aggregate source.

Table 19 Concrete porosity for aggregate source with compressive strength

Aggregate	Porosity (%)	Compressive Strength (MPa)
Blue Rock	32.3	5.7
Blue Rock	27.3	9.4
Blue Rock	22.3	16.6
Blue Rock	17.3	24.8
Newmarket	29.5	7.6
Newmarket	24.5	11.1
Newmarket	19.5	16.2
Newmarket	14.5	25.0
BFS	29.6	4.5
BFS	24.6	6.8
BFS	19.6	9.5
BFS	14.6	15.3
SLA	30.5	5.3
SLA	25.5	7.3
SLA	20.5	11.0
SLA	15.5	16.3
RCA	33.4	5.9
RCA	28.4	9.5
RCA	23.4	15.8
RCA	18.4	25.0

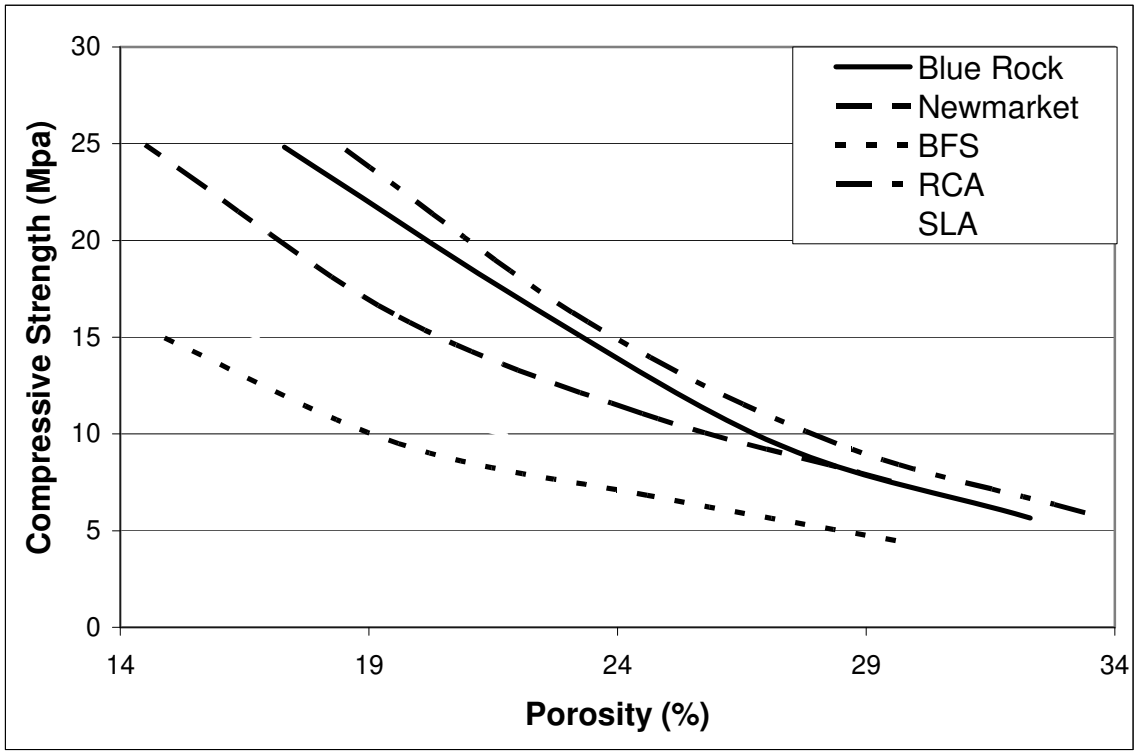

Figure 55 Compressive strength versus concrete porosity for aggregate source

As shown above the aggregate sources seem to follow similar trends to that of porosity and flexural strength, but appear to follow a second order polynomial rather than a linear tendency. Again, the angular aggregates have higher strengths at a given porosity, than that of the angular materials.

CHAPTER 4

SUMMARY AND CONCLUSIONS

As the title of the research states, "Improving the Sound Absorbing Capacity of Portland Cement Concrete Pavements Using Recycled Materials", the goal of this research has been met. The porous PCC pavement mixtures developed have improved the sound absorbing capacity over that of conventional PCC pavement. These mixtures included the use of various recycled aggregates. A procedure has been developed to assist transportation agencies in implementing the use of porous PCC pavements. The procedure is simple and does not extend beyond the abilities of the laboratories supporting those agencies. The procedure is outlined below:

1. Determine what frequency to mitigate (≈1,000 Hz)
2. Select an aggregate source (conventional or recycled)
3. Use the simplex centroid model to examine the aggregate porosity for the aggregate source blends.
4. Determine appropriate mixture design, seeking concrete porosity between 15-25 percent.
5. Evaluate samples for sound absorption (i.e. pavement depth, porosity, etc.) and flexural strength.
6. Adjust mixture design to optimize sound absorption and flexural strength.

The ability for a transportation to evaluate the sample for the sound absorbing capabilities is very important. With ever-increasing construction costs and tighter budgets, the cost

associated with purchasing the impedance tube equipment described in ASTM E1050 is not practical, however the UNH impedance tube is an acceptable economical alternative. For fewer than four hundred dollars and a few other off the shelf pieces of equipment, a material can be examined for its sound absorbing capabilities. The impedance tube is not limited to PCC pavements, but also hot bituminous pavements and base material can also be evaluated. This equipment could also be utilized to evaluate acoustical performance of sound walls as well as pavements.

The following conclusions apply to the aggregates evaluated in this study and may or may not apply to similar aggregates. It can be concluded from the results obtained in this research that:

- As sample depth increases for one and two-layer pavement the frequency at which peak absorption occurs decreases.
- For a two-layer pavement as the top layer thickness increases the absorption coefficient increases to a point, but then rapidly decreases.
- For the aggregate sources evaluated the frequency at which peak absorption occurs increases with porosity.
- For as above aggregate sources the absorption coefficient increases with porosity.
- For as above aggregate sources pulse velocity decreases as porosity increases.
- For as above sources the flexural strength decreases as porosity increases.
- For as above aggregate sources the compressive strength decreases as porosity increases.

CHAPTER 5

RECOMMENDATIONS

The objective of the research was met, however for a porous PCC pavement to become another tool to mitigate pavement noise further analysis needs to be focused on improving the flexural strength of the porous PCC pavement. Other factors that need to be addressed, but not limited to, are skid resistance, freeze-thaw durability, chloride resistance, and constructability.

Another application in which a porous PCC pavement may be beneficial is an overlay on an existing PCC pavement. Porous PCC pavements are the wave of the future and have already been used in Europe for a number of years. With the population moving closer and closer to major highways pavement noise will need alternatives to combat this issue.

REFERENCES

1. Organization of Economic Co-operation and Development, Paris France, 1986.

2. Descornet, G. et al., "*Traffic Noise and Road Surfaces: State of the Art",* Belgian Road Research Centre: Brussels, Belgium, 2000.

3. Davis, J., "*Quiet Asphalt – A Choice for the Future*", Asphalt Magazine, 3 March 2006 <http://www.asphaltmagazine.com/news_archive.

4. McNerney, M.T., et al., "*Comparative Field Measurements of Tire Pavement Noise of Selected Texas Pavement",* Center of Transportation Research: Austin, TX, 1997.

5. Sakamoto, I., et al., "*Tire Noise Reduction by Using Sound Absorbing Material*", Internoise: Fort Lauderdale, FL, 1999.

6. Sandberg, U., "*Six Decades of Vehicle Noise Abatement – But What Happened to the Tyres",* Proceedings of the Institute of Acoustics; Sweden, 1983.

7. Berengier, M., and Anfosso-Ledee, F., "*State of the Art on the Prediction and Control of the Road Traffic Noise in Franc",* Bouguenais, France, 1997.

8. Graf, R.A.G., et al., "*Horn Amplification at a Tyre/Road Interface – Part I: Experiment and Computation*", Internoise: Fort Lauderdale, FL, 1999.

9. Wayson, R.L., "*Relationship Between Pavement Surface Texture and Highway Traffic Noise*", TRB: Synthesis of Highway Practice 268: National Academy Press Washington, D.C., 1998.

10. Jaeckel, J.R., et al., "*Noise Issues of Concrete Pavement Texturin",* TRB 79th Annual Meeting: Washington, D.C., 2000.

11. Sandberg, U., and Ejsmont, J.A., *Texturing of Cement Concrete Pavements to Reduce Traffic Noise Emissions*", TRB 77th Annual Meeting: Washington, D.C., 1998.

12. Saad, Z., et al., "*Design of a Randomized Tining Rake for PCC Pavements Using Spectral Analysis",* TRB 79th Annual Meeting: Washington, D.C., 2000.

13. Descornet, G., et al., "*Concrete Paving Texture",* Britpave seminar: Meriden, 1991.

14. Federal Highway Administration, "*Tire Pavement Noise and Safety Performance*", PCC Surface Texture Technical Working Group: FHWA-SA-96-068, 1996.

15. Watts, G.R., "*The Combined Effects of Porous Asphalt Surfacing and Barriers on Traffic Noise*", Internoise: Liverpool, 1996.Zetterling, T., and Nilsson, N.A. "*Implementation of the Poro-elastic Road Surface",* International Tyre/Road Conference: Gothenburg, SE, 1990.

16. Storeheier, S.A., and Arnevik, A., "*Traffic Noise Reduction through the Optimisation of Void Distribution in Road Binder Layer and Wearing Course",* International Tyre/Road Conference: Gothenburg, SE, 1990.

17. Sandberg, U., and Walker, B., "*Conclusions form Session V – Exposed Aggregate Concrete",* The PIARC-workshop, Noise reducing concrete surfaces: Vienna, 1992.

18. Onstenk, E., et al., "*Laboratory Study of Porous Concrete for its use as Top-Layer of Concrete Pavements*", Concrete Pavement Design and Rehabilitation Volume 2, 1992.

19. Woodside, A.R., et al., "*The Optimization of Porous Asphalt Road Surfaces to Maximise Sound Absorption",* Internoise: Fort Lauderdale, FL, 1999.

20. Steven, H., "*Recent German Experience with Open-Pored Surfacing*", International Tyre/Road Conference: Gothenburg, SE, 1990.

21. ASTM C29, "*Standard Test Method for Bulk Density ("Unit Weight") And Voids In Aggregate*", American Society for Testing and Materials, Book of Standards: 4.02, West Conshohocken, PA, 2001.

22. ASTM C127, "*Standard Test Method For Density, Relative Density (Specific Gravity), And Absorption Of Coarse Aggregate*", American Society for Testing and Materials, Book of Standards: 4.06, West Conshohocken, PA, 2001.

23. ASTM C384, "*Standard Test Method for Impedance and Absorption of Acoustical Materials by Impedance Tube Method*", American Society for Testing and Materials, Book of Standards: 4.06, West Conshohocken, PA, 2001.

24. ASTM C597, "*Standard Test Method for Pulse Velocity Through Concrete*", American Society for Testing and Materials, Book of Standards: 4.02, West Conshohocken, PA, 2001.

25. ASTM C78, "*Standard Test Method for Flexural Strength of Concrete (Using Simple Bean with Third-Point Loading*", American Society for Testing and Materials, Book of Standards: 4.02, West Conshohocken, PA, 2001.

26. ASTM C39, "*Standard Test Method for Compressive Strength of Cylindrical Concrete Specimens*", American Society for Testing and Materials, Book of Standards: 4.02, West Conshohocken, PA, 2001.

27. ASTM C457, "*Standard Test Method for Microscopical Determination of Parameters of the Air-Void System in Hardened Concrete*", American Society for Testing and Materials, Book of Standards: 4.02, West Conshohocken, PA, 2001.

28. ASTM E1050, "*Standard Test Method for Impedance and Absorption of Acoustical Materials Using A Tube, Two Microphones and A Digital Frequency Analysis System*", American Society for Testing and Materials, Book of Standards: 4.06, West Conshohocken, PA, 2001.

29. Kashi, M., et al., "*Synthetic Lightweight Aggregate for Highway Construction*", Recycled Materials Research Center: Durham, NH 2001.

30. Pitre, J., Gress, D., and Magee, B., "*Improving the Sound Absorbing Capacity of Portland Cement Concrete Pavements Using Recycled Materials*" Recycled Materials Research Center: Beneficial Use of Recycled Materials in Transportation Applications: Arlington, VA, 2001.

APPENDIX

POROUS PCC PAVEMENT PROCEDURE

The following is a description of the procedure to develop porous PCC pavements:

- Select an aggregate source.
- Separate aggregate into sizes retained on 2.36 mm, 4.75 mm, and 9.5 mm sieves.
- If specified sizes are not available, crush and pulverize to achieve the desired sizes.
- Setup statistical model to predict aggregate porosity by using the following blends:
    - 100 percent by weight 2.36 mm
    - 100 percent by weight 4.75 mm
    - 100 percent by weight 9.5 mm
    - 50/50 percent by weight 2.36 mm and 4.75 mm
    - 50/50 percent by weight 2.36 mm and 9.5 mm
    - 50/50 percent by weight 4.75 mm and 9.5 mm
    - 33/33/33 percent by weight 2.36 mm, 4.75 mm, and 9.5 mm
    - 33/33/33 percent by weight 2.36 mm, 4.75 mm, and 9.5 mm
    - 33/33/33 percent by weight 2.36 mm, 4.75 mm, and 9.5 mm
- Blend aggregate in mixer.
- Run above trials according to modified ASTM C29.
- Determine porosity for aggregate blends.

- Model data using statistical software (JMP IN ™) using four variables, fraction of 2.36 mm aggregate, fraction of 4.75 mm aggregate, fraction of 9.5 mm aggregate, and porosity.
- Determine best fit for data using statistical software (i.e. full factorial, response surface, etc.) by examining R^2 values for each model.
- From porosity results determine cement paste content to achieve desired concrete porosity (≈ 20 percent) and use porosity equation to determine fractions of aggregate sizes.
- Determine quantity of concrete required for desired tests (i.e. impedance tube, flexural strength, compressive strength, etc.) and make necessary cylinders and beams. Enough samples should be created to compare the samples acoustically by varying sample depth, porosity, etc.
- Find an area with enough space to setup impedance tube and away from large electrical equipment, which may generate stray electrical interference.
- Construct impedance tube using the following materials
    - 101 mm diameter by 2.5 m pvc pipe
    - 6.25 mm diameter by 1.5 metal tubing
    - 5 to 7 mm diameter microphone
    - 80 to 90 mm diameter speaker with at least 25 watts of power
    - Scale
    - Fiberglass insulation
    - Amplifier
    - Oscilloscope
    - Frequency generator
    - Frequency filter
    - Switch
    - Reference material (i.e. ultra high density polyethylene, etc.)

- Connect microphone to end of metal tube running wires through the tube to the switch, then from the switch connect to the frequency filter, from the frequency filter connect to the oscilloscope.
- Connect the frequency generator to the frequency filter and the amplifier, from the amplifier connect the speaker.
- Setup pvc pipe with stop for sample and one end, then adjust scale on the other end to measure distance from stop, which will be face of sample.
- Slide metal tube with microphone inside on the bottom of the pvc pipe.
- Place speaker inside pvc pipe on the scale side with fiberglass insulation in front of it.
- Calibrate setup using reference material.
    - Turn on all equipment.
    - Adjust volume on amplifier as high as the speaker can handle without distorting the signal.
    - Set frequency generator to a frequency between 500 and 1,000 Hz.
    - Maximize signal by adjusting frequency filter.
    - Slide metal tube away from the sample/reference face and record peak from the oscilloscope. Profile the signal from reference/sample face and compare to theoretical profile. Verify that maximum and minimums occur at theoretical positions based on set frequency.
    - Test reference sample and ensure material is very close to being 100 percent reflective.

- Test samples in impedance tube and record maximum and minimums for given frequencies between 300 and 1,500 Hz. At points were significant changes occur take more measurements around the change to ensure profile is thoroughly recorded. Maximize signal using frequency filter for each frequency.
- Calculate absorption coefficient from results and plot it against the frequency.

- Determine peak absorption coefficient and what frequency it occurs from the plots.
- Compare peak absorption and frequency at which it occurs among samples.
- Determine other properties (i.e. flexural strength, etc.) using ASTM standards.
- Optimize mixture by utilizing acoustical and other desired properties.